

Starch Granule Biosynthesis in *Arabidopsis* Is Abolished by Removal of All Debranching Enzymes but Restored by the Subsequent Removal of an Endoamylase

Sebastian Streb,^a Thierry Delatte,^{a,1} Martin Umhang,^a Simona Eicke,^a Martine Schorderet,^b Didier Reinhardt,^b and Samuel C. Zeeman^{a,2}

^a Institute of Plant Sciences, ETH Zurich, CH-8092 Zurich, Switzerland

^b Department of Plant Biology, University of Fribourg, CH-1700 Fribourg, Switzerland

Several studies have suggested that debranching enzymes (DBEs) are involved in the biosynthesis of amylopectin, the major constituent of starch granules. Our systematic analysis of all DBE mutants of *Arabidopsis thaliana* demonstrates that when any DBE activity remains, starch granules are still synthesized, albeit with altered amylopectin structure. Quadruple mutants lacking all four DBE proteins (Isoamylase1 [ISA1], ISA2, and ISA3, and Limit-Dextrinase) are devoid of starch granules and instead accumulate highly branched glucans, distinct from amylopectin and from previously described phytyloglycogen. A fraction of these glucans are present as discrete, insoluble, nanometer-scale particles, but the structure and properties of this material are radically altered compared with wild-type amylopectin. Superficially, these data support the hypothesis that debranching is required for amylopectin synthesis. However, our analyses show that soluble glucans in the quadruple DBE mutant are degraded by α - and β -amylases during periods of net accumulation, giving rise to maltose and branched malto-oligosaccharides. The additional loss of the chloroplastic α -amylase AMY3 partially reverts the phenotype of the quadruple DBE mutant, restoring starch granule biosynthesis. We propose that DBEs function in normal amylopectin synthesis by promoting amylopectin crystallization but conclude that they are not mandatory for starch granule synthesis.

INTRODUCTION

Starch is the predominant storage carbohydrate in higher plants and is a key renewable resource for humankind as both food and an industrial raw material. Despite the importance of starch, there are major gaps in our understanding of its biosynthesis. Starch is composed of glucose polymers (amylopectin and amylose) and occurs as semicrystalline granules inside plastids (chloroplasts in leaves and amyloplasts in storage tissues). In amylopectin, which typically accounts for 70% or more of the granule mass, glucosyl residues are linked by α -1,4-bonds to form chains that are branched via α -1,6-bonds (Buléon et al., 1998; Zeeman et al., 2007). Branch points occur with a frequency of 1 in 20 to 25 glucose residues and are positioned in a nonrandom pattern resulting in clusters of adjacent, linear chains (a racemose-like structure). In the widely accepted model for amylopectin structure, the adjacent linear sections of the chains

interact to form double helices, which then pack into stable, semicrystalline lamellae, repeated with a 9-nm periodicity (see Supplemental Figure 1 online). However, neither the precise architecture of amylopectin nor the ways in which the starch biosynthetic enzymes act in concert to produce it are fully understood.

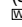
The elongation of α -1,4-linked chains is catalyzed by starch synthases, which transfer the glucosyl moiety of ADP-Glc to the nonreducing end of an existing chain. Branch points are introduced by branching enzymes, which catalyze a glucanotransferase reaction whereby part of an existing α -1,4-linked chain is transferred to the C6 position of a glucosyl residue of another chain. Both starch synthases and branching enzymes occur as multiple isoforms with distinct properties, each thought to fulfill a specific role in amylopectin biosynthesis (for review, see Tomlinson and Denyer, 2003). There is also strong evidence that debranching enzymes (DBEs), which hydrolyze α -1,6-branch points, are involved in the production of amylopectin (for reviews, see Ball et al., 1996; Myers et al., 2000; Zeeman et al., 2007).


Plants and green algae contain two classes of DBEs: isoamylase (ISA) and limit-dextrinase (LDA; also called pullulanase). Both classes hydrolyze α -1,6-branch points but differ in their substrate specificity, notably the ability of LDA, but not ISA, to act on the fungal polysaccharide pullulan (maltotriosyl units linked end-to-end by α -1,6-bonds). The ISA class can be divided into three subfamilies designated ISA1, ISA2, and ISA3 (Hussain et al., 2003; Rahman et al., 2003). *Arabidopsis thaliana* has one

¹ Current address: Department of Pharmaceutical Sciences, University of Utrecht, Sorbonnelaan 16, 3584CA Utrecht, The Netherlands.

² Address correspondence to szeeman@ethz.ch.

The author responsible for distribution of materials integral to the findings presented in this article in accordance with the policy described in the Instructions for Authors (www.plantcell.org) is: Samuel C. Zeeman (szeeman@ethz.ch).

 Online version contains Web-only data.

 Open Access articles can be viewed online without a subscription. www.plantcell.org/cgi/doi/10.1105/tpc.108.063487

gene encoding each ISA subfamily member and one gene encoding LDA. Mutation or repression of the genes encoding ISA1 proteins results in a reduction in granular starch in developing endosperms of maize (*Zea mays*), rice (*Oryza sativa*), and barley (*Hordeum vulgare*) (James et al., 1995; Nakamura et al., 1997; Burton et al., 2002), in *Chlamydomonas* cells (Mouille et al., 1996; Dauvillée et al., 2001; Posewitz et al., 2004), in *Arabidopsis* leaves (Zeeman et al., 1998b; Delatte et al., 2005; Wattedled et al., 2005), and in potato (*Solanum tuberosum*) tubers (Bustos et al., 2004). In all cases, starch granules are partly replaced by a water-soluble polymer with characteristics similar to glycogen (thus termed phytoglycogen). Compared with amylopectin, phytoglycogen has relatively more short chains with a degree of polymerization (d.p.) less than 10 and contains more branch points, which are positioned closer together.

A complete picture of DBE function for a single species is still missing, but most is known for *Arabidopsis*. Mutation of *ISA2* eliminates the same enzyme activity as mutation of *ISA1*, and the mutant phenotypes are indistinguishable from each other (Delatte et al., 2005; Wattedled et al., 2005). This is consistent with previous observations that isoamylases exist as multimeric enzymes (Ishizaki et al., 1983; Fujita et al., 1999; Dauvillée et al., 2001), which in potato and rice have been shown to contain both *ISA1* and *ISA2* (Bustos et al., 2004; Utsumi and Nakamura, 2006). The loss of *ISA3* or *LDA* alone does not lead to phytoglycogen production (Wattedled et al., 2005; Delatte et al., 2006). The *isa3* mutant has a starch-excess phenotype and reduced rates of starch mobilization in leaves (Wattedled et al., 2005; Delatte et al., 2006). Although *Ida* mutants have normal starch metabolism, loss of *LDA* in the *isa3* background enhances the severity of the starch-excess phenotype, showing that *LDA* contributes to starch degradation when *ISA3* is missing (Delatte et al., 2006). Maize *Ida* mutants (*zpu1*) display slightly elevated starch levels in leaves and a reduced rate of endosperm starch mobilization during seedling establishment (Dinges et al., 2003). These data suggest that *ISA3* and *LDA* function primarily in starch breakdown. However, it has been reported that the loss of *LDA* enhances the phytoglycogen-accumulating phenotype of *ISA* mutants in different species (Kubo et al., 1999; Dinges et al., 2003; Wattedled et al., 2005).

Models to explain phytoglycogen accumulation in *isa1* mutants have proposed that debranching is an integral or even mandatory step in starch biosynthesis (Ball et al., 1996; Myers et al., 2000; Zeeman et al., 2007). It is envisioned that wrongly positioned branch points introduced by branching enzymes are removed, thereby allowing the formation of semicrystalline lamellae. The presence of some starch granules in most *isa1* mutants suggests either that *ISA3* and *LDA* can partially compensate for the loss of *ISA1* or that debranching is facilitatory, but not mandatory, for granule biosynthesis. It is also possible that other glucan-metabolizing enzymes present during biosynthesis can contribute to determining glucan structure. For example, Delatte et al. (2005) observed that maltose (a product of amylolysis) accumulates concurrently with phytoglycogen in *Arabidopsis isa1* mutants. This led them to suggest that secondary modification of nascent amylopectin molecules by amylases could influence whether these molecules go on to form starch granules or remain soluble as phytoglycogen.

The aim of the work presented here was to determine the role of each DBE in starch granule biosynthesis and whether debranching is a mandatory step. We also sought to determine the extent to which amylases affect glucan structure. We present a phenotypic comparison of the glucans accumulated in the double, triple, and quadruple DBE mutants of *Arabidopsis*. The phenotype of the DBE-free quadruple mutant is consistent with the idea that debranching is indeed mandatory for amylopectin synthesis. However, we show that other hydrolytic enzymes have a major influence on glucan structure in the absence of DBEs and demonstrate that the additional removal of an endoamylase allows starch granule synthesis to occur in the absence of DBEs.

RESULTS

Production of Double, Triple, and Quadruple DBE Mutants

Current evidence suggests that the four *Arabidopsis* genes encoding DBE-like proteins produce three active enzymes, because *ISA1* and *ISA2* are proposed to form a single heteromultimeric holoenzyme (Hussain et al., 2003; Delatte et al., 2005; Wattedled et al., 2005). Thus, multiple mutants lacking *ISA1*, *ISA2*, or both should be equivalent with respect to their phenotype (e.g., *isa1/isa3*, *isa2/isa3*, and *isa1/isa2/isa3* should all be equivalent). However, we created and analyzed all possible combinations of the four mutants to control for unexpected phenotypic differences. Segregating F2 populations derived from crosses between mutants were screened using PCR to identify plants with homozygous mutations in each gene. The details for the selected mutants and primer sequences used for genotyping are given in Supplemental Table 1 online. Native gel analyses revealed that there were no major changes in starch synthase and branching enzyme activities in a selection of the mutant combinations (see Supplemental Figure 2 online).

We conducted an experiment to determine the amount of glucan in several of the mutant combinations. In wild-type plants, starch is synthesized throughout the day and almost completely degraded during the subsequent night. Therefore, we initially measured insoluble and soluble glucans at the end of the day and the end of the night. Insoluble glucans includes starch granules or other particulate glucans pelleted by centrifugation at 3000g, while soluble glucans includes phytoglycogen and smaller oligosaccharides. Extracts were made using perchloric acid to inactivate immediately enzymes that might degrade the glucans (Delatte et al., 2005). We compared the *isa1/isa2* double mutant, the *isa1/isa2/lda* and *isa1/isa2/isa3* triple mutants, and the quadruple DBE mutant to determine the effect of the additional loss of *LDA* and/or *ISA3* on the glucan-accumulating phenotype of *isa1/isa2*. We also analyzed the *isa3* and *lda* single mutants and the *isa3/lda* double mutant for comparison (Figure 1A).

As expected, the wild type contained significant amounts of starch at the end of the day (10.9 mg/g fresh weight), 90% of which was degraded during the subsequent night. The *isa1/isa2* double mutant contained both insoluble and soluble glucans in a ratio of ~2:5 (a total of 7.5 mg/g fresh weight). The *lda* mutant contained wild-type levels of insoluble glucan, whereas the levels

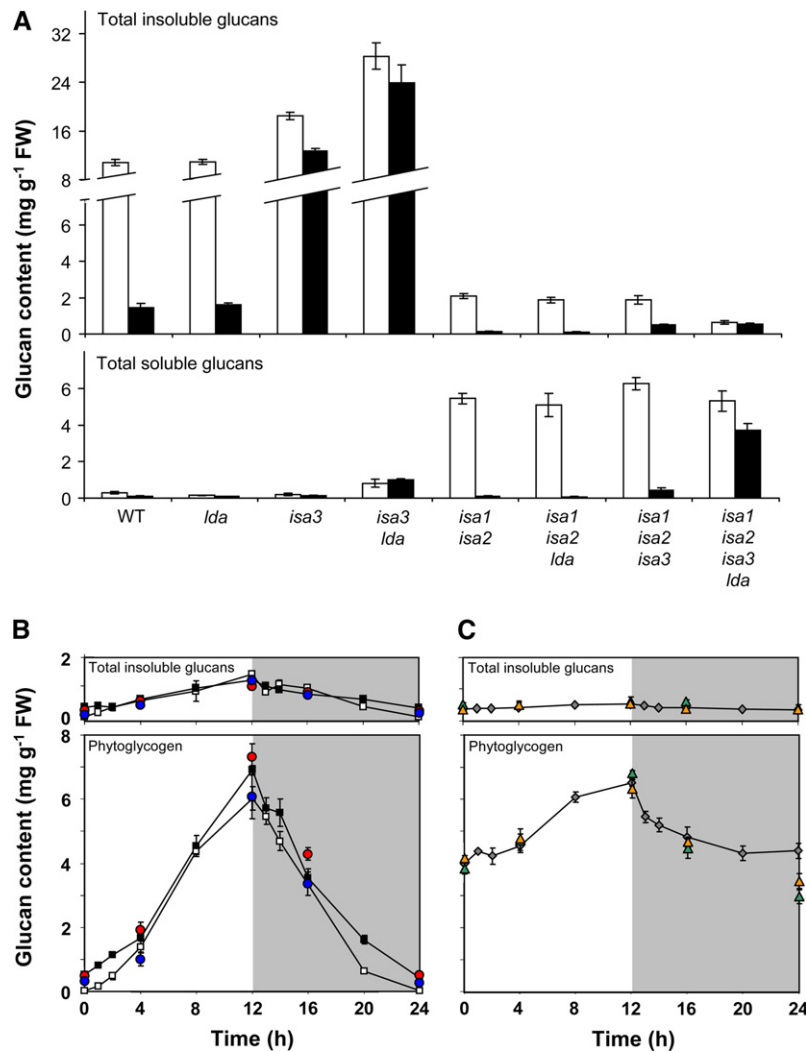


Figure 1. Quantification of Insoluble and Soluble Glucans in Wild-Type and DBE Mutant Plants.

Plants were harvested and immediately frozen in liquid N₂. Each sample comprised all of the leaves from a single plant (A) or complete individual rosettes (B) and (C). Total insoluble and soluble glucans were extracted using perchloric acid, and glucans were measured after enzymatic hydrolysis to glucose. FW, fresh weight.

(A) Total insoluble (top) and soluble (bottom) glucans from wild-type and DBE mutant plants harvested at the end of a 12-h photoperiod (white bars) or at the end of the night (black bars). Each value is the mean ± SE of eight replicate samples. Note the change of scale on the y axis.

(B) Total insoluble glucan and phytoglycogen precipitated from the soluble fraction of *isa1/isa2* (white squares), *isa1/isa2/isa3* (black squares), *isa1/isa3* (red circles, no line), and *isa2/isa3* (blue circles, no line). Each point is the mean ± SE from four replicate samples. Wild-type plants grown in parallel had 7.4 ± 0.2 and 0.6 ± 0.0 mg starch/g fresh weight at the end of the day and the end of the night, respectively.

(C) Total insoluble glucan and phytoglycogen precipitated from the soluble fraction of the *isa1/isa2/isa3/lda* quadruple mutant (gray diamonds). Additional data are given for *isa1/isa3/lda* (green triangles, no line) and *isa2/isa3/lda* (gold triangles, no line). Each point is the mean ± SE from four replicate samples.

were elevated in the *isa3* mutant and the *isa3/lda* double mutant. Furthermore, *isa3/lda* contained small amounts of soluble glucans, shown previously to be soluble branched oligosaccharides rather than phytoglycogen (Delatte et al., 2006). The triple mutant *isa1/isa2/lda* contained the same amounts of insoluble and soluble glucans as *isa1/isa2*, and all glucans made during the day were mobilized at night. Similarly, the triple isoamylase

mutant *isa1/isa2/isa3* produced the same amounts of insoluble and soluble glucans as *isa1/isa2*, most of which was degraded during the night, although slightly more glucan remained at the end of the night than in *isa1/isa2*. Thus, either ISA3 or LDA can debranch insoluble and soluble glucans during degradation. The quadruple mutant had a very distinct phenotype, containing less insoluble glucan than *isa1/isa2* at the end of the day but

comparable amounts of soluble glucan. At the end of the night, the amount of soluble glucan declined by only 30%. The insoluble glucan content decreased only slightly, if at all.

Diurnal Changes in Insoluble and Soluble Glucans Synthesized in DBE Mutant Combinations

We determined the pattern of accumulation of insoluble glucan and phytoglycogen (defined here as the methanol-precipitable soluble glucan) over the course of a 24-h diurnal cycle in selected mutant combinations. The initial results in Figure 1A did not reveal a change in the insoluble-to-soluble glucan ratio upon loss of LDA in addition to ISA1 and ISA2. This contrasts with the situation in maize endosperm (Dinges et al., 2003) and previous observations in *Arabidopsis* (Wattebled et al., 2005), where loss of LDA was reported to increase the ratio of phytoglycogen to starch. We compared the *isa1/lda* double mutant with *isa1* and the *isa2/lda* double mutant with *isa2*. The amounts of insoluble glucan and phytoglycogen were very similar among all four lines, suggesting that in *Arabidopsis* the additional loss of LDA has little or no impact on the phenotype of the *isa1* and *isa2* mutants (see Supplemental Figure 3 online).

The pattern of glucan accumulation and degradation throughout the diurnal cycle in the isoamylase triple mutant (*isa1/isa2/isa3*) was also similar to that of the *isa1/isa2* double mutant (Figure 1B). As in our first experiment, almost all of the glucan made during the day was degraded at night. Similar results were obtained for the two double mutants, *isa1/isa3* and *isa2/isa3* (Figure 1B). This is intriguing, as *isa3* single mutants have slower rates of starch breakdown at night than the wild type, which leads to an imbalance between glucan accumulation and degradation and the development of a starch-excess phenotype (Delatte et al., 2006). Unlike the other mutant combinations, the quadruple DBE mutant had appreciable amounts of glucans throughout the day and night (Figure 1C). The low level of insoluble glucan did not change, whereas the amount of phytoglycogen increased gradually during the day and decreased rapidly in the first few hours of the night. At the end of the night, only one-third of the phytoglycogen had been mobilized. Similar results were obtained for the two triple mutants, *isa1/isa3/lda* and *isa2/isa3/lda* (Figure 1C). We conducted a second experiment in which we extended the length of the night by 48 h, but there was no further decrease in the phytoglycogen content of the quadruple DBE mutant compared with the end of the night.

Glucan Structure Is Radically Altered in the Absence of all DBEs

Although the amounts of insoluble and soluble glucans did not change substantially upon loss of either ISA3 or LDA in addition to ISA1 and ISA2, we analyzed the chain length distributions to determine if the structure was altered in either case. When compared with wild-type amylopectin, the glucans in *isa1/isa2* and *isa3* have altered chain length distributions (Figure 2) (Delatte et al., 2005, 2006), whereas LDA does not (data not shown) (Delatte et al., 2006). The chain length distributions of the

insoluble glucans and phytoglycogen from the *isa1/isa2/lda* triple mutant were the same as those from *isa1/isa2*. Similarly, no differences were detected between the glucans from the *isa1/lda* double mutant and *isa1* or the glucans from the *isa2/lda* double mutant and *isa2* (see Supplemental Figures 4 and 5 online). These data indicate that loss of LDA in addition to ISA1 and ISA2 does not alter glucan structure.

By contrast, the proportion of very short chains (d.p. 3 to 5) in both the insoluble glucans and the phytoglycogen from the isoamylase triple mutant was significantly elevated compared with the *isa1/isa2* mutant (Figure 2). When compared with wild-type amylopectin, the changes in the chain length distributions of *isa1/isa2* and *isa3* are combined in the triple isoamylase mutant. This indicates that the isoamylase enzymes have distinct specificities *in vivo*, consistent with the analysis of their properties *in vitro* (Hussain et al., 2003; Takashima et al., 2007). However, unlike the *isa3* single mutant, there is very little glucan present at the end of the night in the triple isoamylase mutant (Figures 1A and 1B). Thus, these data show that ISA3 actively removes very short chains from the glucans that are synthesized during the day in the *isa1/isa2* background. As branching enzymes are not thought to produce very short chains (Borovsky et al., 1975; Guan and Preiss, 1993; Takeda et al., 1993), they most likely arise through α - or β -amylolysis of longer chains. Similar analyses were conducted on the two double mutants, *isa1/isa3* and *isa2/isa3*. In both cases, the results were similar to those observed with the isoamylase triple mutant (see Supplemental Figure 6 online).

The glucans from the quadruple mutant plants were radically altered compared with wild-type amylopectin and the glucans of the mutants analyzed thus far (Figure 2). The chain length profiles were dominated by chains with d.p. < 10, with d.p. 3 being the most abundant. This was true for both the insoluble glucans and phytoglycogen. The differences between the chain length distributions of the phytoglycogens and wild-type amylopectin were slightly more extreme than those of the insoluble glucans (compare Figures 2B and 2C). Similar analyses were conducted on the two triple mutants, *isa1/isa3/lda* and *isa2/isa3/lda*. In both cases, the results were similar to those observed with the quadruple DBE mutant (see Supplemental Figure 6 online).

The dominance of short chains in the glucans extracted from the quadruple mutant means that most chains would be too short to form the double helical structures typically associated with amylopectin. Therefore, it was surprising that some (0.3 to 0.5 mg/g fresh weight) of the glucan accumulated in the quadruple mutant was insoluble (i.e., pelleted by centrifugation at 3000g for 10 min). To exclude that this was an artifact arising from the contamination of the insoluble material (e.g., coprecipitation of soluble glucans with proteins during perchloric acid extraction), we performed a series of control experiments. First, the insoluble pellet was rehomogenized and washed three times in water. This did not result in the release of additional soluble glucan from the pellet of insoluble material. Second, leaves were extracted in nonacidic aqueous medium. Glucans were still observed in the insoluble fraction in similar amounts as in the perchloric acid extracts. Third, the pellets were washed with 1.5% (w/v) SDS. This did not solubilize the insoluble glucan. However, incubation of the insoluble suspension at 95°C for 10 min (a treatment that

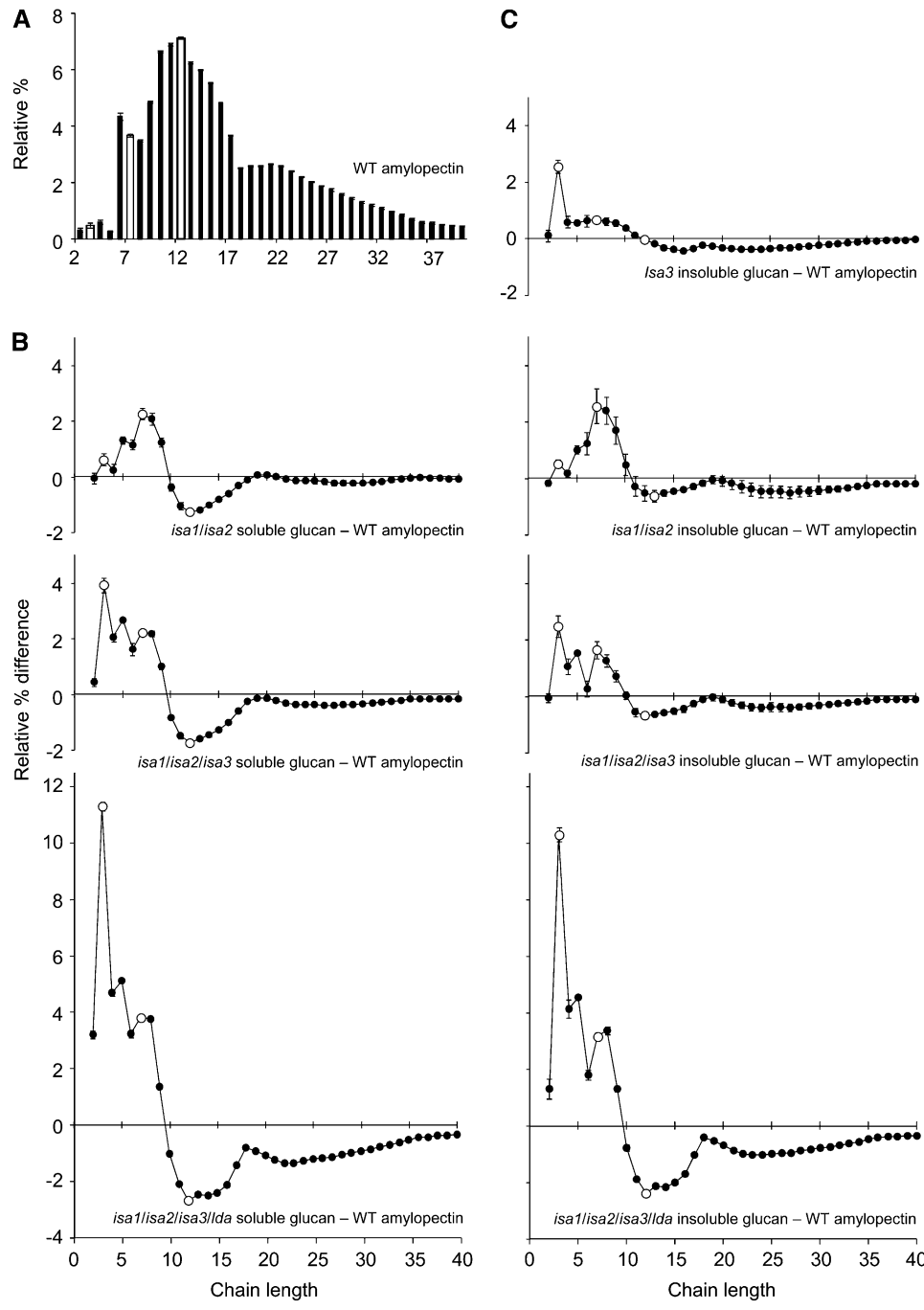


Figure 2. Changes in the Chain Length Distributions of Glucans Extracted from Leaves of the DBE Mutant Combinations.

Glucans extracted from individual plants harvested at the end of the day (phytglycogen precipitated from the soluble extracts and total insoluble glucans) were pooled such that each plant contributed an equal amount of glucan. The resultant samples were debranched with *Pseudomonas* isoamylase and *Klebsiella* pullulanase and analyzed by HPAEC-PAD. Peak areas were summed, and the areas of individual peaks were calculated as a percentage of the total \pm SE of three technical replicates. The difference plots for each of the mutant glucans shown were derived by subtracting the relative percentage values of wild-type amylopectin. For ease of comparison, open symbols are placed at d.p. 3, 7, and 12. The SE values of the compared data sets were added together. Additional data in Supplemental Figure 6 online show the equivalence between the glucans in *isa1/isa3*, *isa2/isa3*, and *isa1/isa2/isa3* and between *isa1/isa3/lda*, *isa2/isa3/lda*, and *isa1/isa2/isa3/lda*.

- (A)** Chain length distribution of wild-type amylopectin.
- (B)** The difference between the chain length distributions of the soluble glucans from the DBE mutant combinations (as indicated) and wild-type amylopectin shown in **(A)**.
- (C)** The difference between the chain length distributions of the insoluble glucans from the DBE mutant combinations (as indicated) and wild-type amylopectin shown in **(A)**.

effectively solubilizes wild-type starch granules) solubilized all of the glucan.

The Quadruple DBE Mutant Contains No Starch Granules

We used electron microscopy to investigate the appearance of the glucans formed in the different mutant combinations. Transmission electron micrographs of the *isa1/isa2* double mutant revealed that mesophyll cell chloroplasts contained predominantly phytoglycogen, whereas epidermal cell plastids and bundle-sheath cell chloroplasts contained visible starch granules (Figure 3) (Delatte et al., 2005). The *isa2/lda* double mutant (equivalent to the *isa1/isa2/lda* triple mutant) was similar to *isa1/isa2*. The triple isoamylase mutant also contained visible starch granules (see Supplemental Figure 7 online). In many cases, these granules appeared smaller, cracked, and fissured compared with the corresponding granules in *isa1/isa2*. By contrast,

the quadruple mutant did not contain any visible starch granules in any of the leaf cell types analyzed (Figure 3; see Supplemental Figure 7 online). Instead, the chloroplasts of all cells contained particles ranging in size from 30 to 100 nm in diameter. As expected, wild-type and *isa1/isa2* mesophyll chloroplasts did not contain visible starch granules and phytoglycogen, respectively, at the end of the night, but the quadruple mutant chloroplasts were still filled with glucan particles (Figure 3), consistent with the quantitative measurements (Figure 1).

To determine if any of the particles observed in the transmission electron micrographs of the quadruple mutant were equivalent to the insoluble material detected in leaf homogenates, we purified the insoluble glucan from the homogenates using a series of wash, filtration, and centrifugation steps (see Methods). Scanning electron microscopy of the resultant insoluble glucans revealed spherical particles up to 100 nm in diameter (Figures 4D and 4E). Pretreatment of the isolated insoluble glucans by

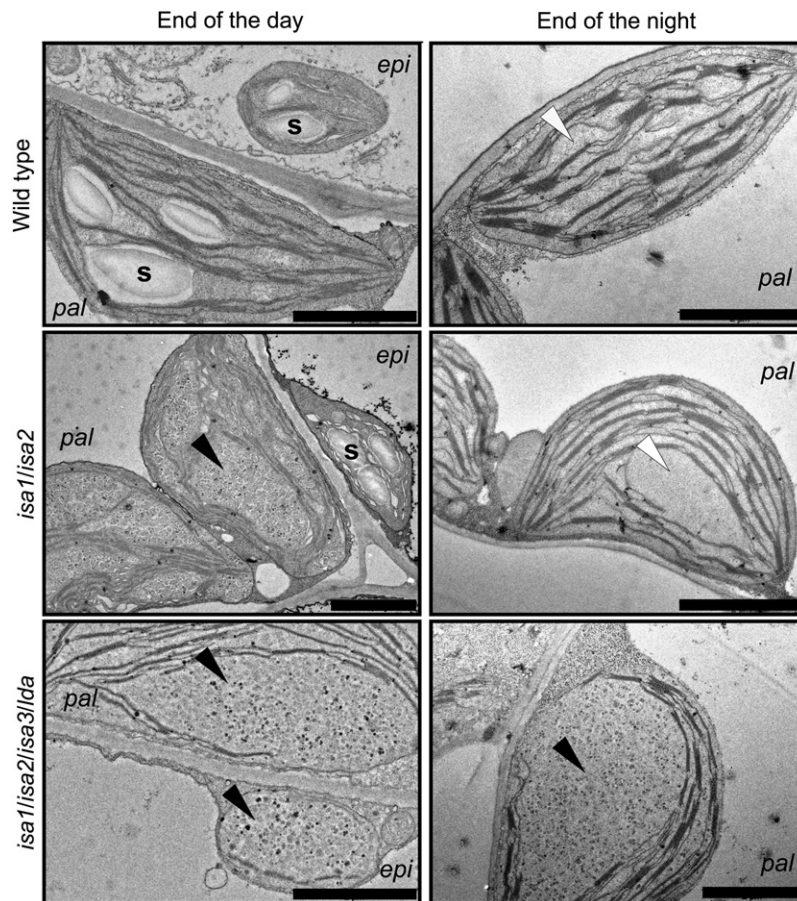


Figure 3. Glucans Accumulating in Leaf Palisade and Adjacent Epidermal Cell Plastids of the Wild Type, the *isa1/isa2* Double Mutant, and the *isa1/isa2/lda* Quadruple Mutant, Visualized by Transmission Electron Microscopy.

Starch granules (s) were present in wild-type plastids and in the epidermal cell plastids of *isa1/isa2*. No starch granules were visible in the quadruple DBE mutant. Soluble glucan and/or particulate material (black arrowheads) are indicated in *isa1/isa2* mesophyll cells and in the quadruple mutant. Note the absence of glucans from wild-type and *isa1/isa2* palisade cell chloroplasts at the end of the night (white arrowheads) but the glucan particles remaining in the quadruple DBE mutant. Additional images from these and other mutants are provided in Supplemental Figure 7 online. pal, leaf palisade cell plastid; epi, epidermal cell plastid. Bars = 2 μ m.

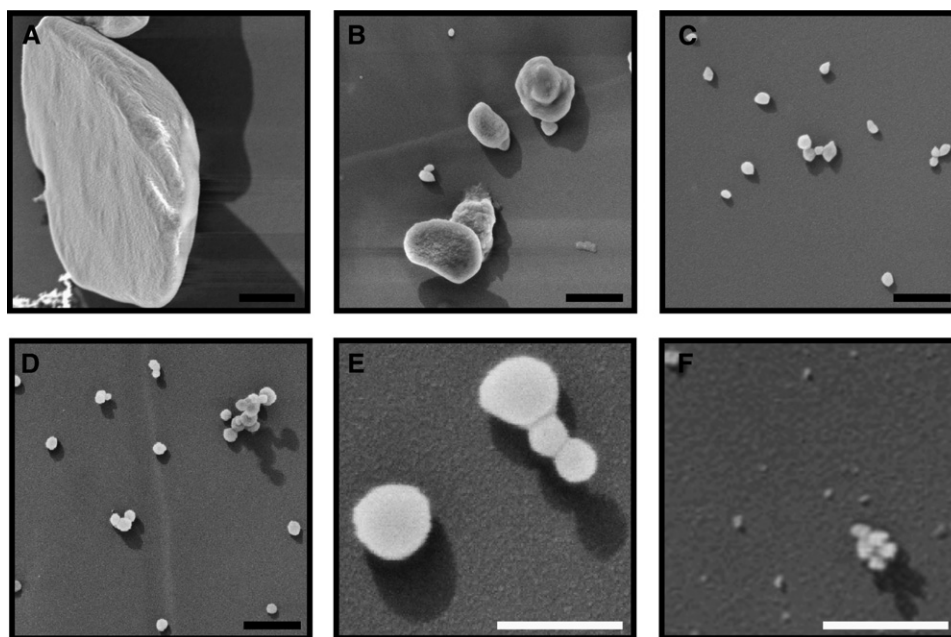


Figure 4. Scanning Electron Micrographs of Insoluble Glucans Isolated from the Wild Type, the *isa1/isa2* Double Mutant, and the Quadruple DBE Mutant.

(A) Starch granule from the wild type.

(B) Starch granules isolated from the *isa1/isa2* double mutant.

(C) Nanoscale insoluble glucan particles isolated from the *isa1/isa2* double mutant.

(D) Nanoscale insoluble glucan particles isolated from the quadruple DBE mutant.

(E) As in (D), at higher magnification.

(F) As in (E), after incubation of the particles in water at 95°C for 10 min. No particles similar to those in (D) and (E) were visible.

Black bars = 500 nm; white bars = 200 nm.

heating to 95°C in water caused the disappearance of the spherical structures (Figure 4F). Similarly, pretreatment of a replicate preparation with α -amylase and amyloglucosidase degraded the insoluble glucans and caused the disappearance of the spherical structures. Interestingly, particles similar in appearance could be purified from the insoluble fraction of *isa1/isa2* extracts in addition to larger, well-defined starch granules (Figures 4B and 4C). Furthermore, particles of a similar size could be observed in the transmission electron micrographs of *isa1/isa2* and the isoamylase triple mutants (Figure 3; see Supplemental Figure 7 online).

We mixed the heat-solubilized glucans from the wild type, *isa1/isa2*, and the quadruple mutant with an iodine solution (Figure 5). The absorption spectrum of the mixture depends on the amount of iodine bound and the type of complex formed with the glucan secondary structures. The λ_{\max} value of the iodine complex with wild-type starch was 560 nm, whereas that of glycogen (from oyster) was 462 nm. The corresponding values of the insoluble glucan and phytyglycogen from *isa1/isa2* were 535 and 490 nm, respectively. The absorption spectra of the insoluble glucan and phytyglycogen from the quadruple mutant (λ_{\max} values of 482 and 466 nm, respectively) were much more similar to that of glycogen than of amylopectin.

We investigated whether the insoluble glucan particles from the quadruple mutant contained other components (e.g., pro-

teins). After solubilization of the glucan, we determined the protein content, either via the Bradford method (Bradford, 1976) or via the ninhydrin method (Starcher, 2001). With both methods, the protein content was below the limit of detection (determined to be 0.3% [w/w] of the glucan added to these assays, using BSA as a standard). Similarly, the protein content of wild-type starch granules and *isa1/isa2* insoluble glucans was below the limit of detection. We also analyzed the unheated material using Fourier transformed infrared (FTIR) spectroscopy. The resultant spectrum (see Supplemental Figure 8 online) contained peaks characteristic of α -1,4- and α -1,6-linked polyglucans (Capron et al., 2007) and were broadly similar to those obtained with wild-type starch and the insoluble glucans from the *isa1/isa2* double mutant. The spectra lacked peaks that would indicate the presence of abundant proteins.

In the Absence of DBEs, Extensive Turnover by α - and β -Amylases Influences Glucan Structure

We measured low molecular weight malto-oligosaccharides to investigate the extent to which amylases act on the glucans synthesized in the absence of DBEs. In all quadruple mutant samples, most of the soluble glucan (60 to 70%) was phytyglycogen and could be precipitated in 75% (v/v) methanol. However, a significant fraction (30 to 40%) could not be precipitated (Figure

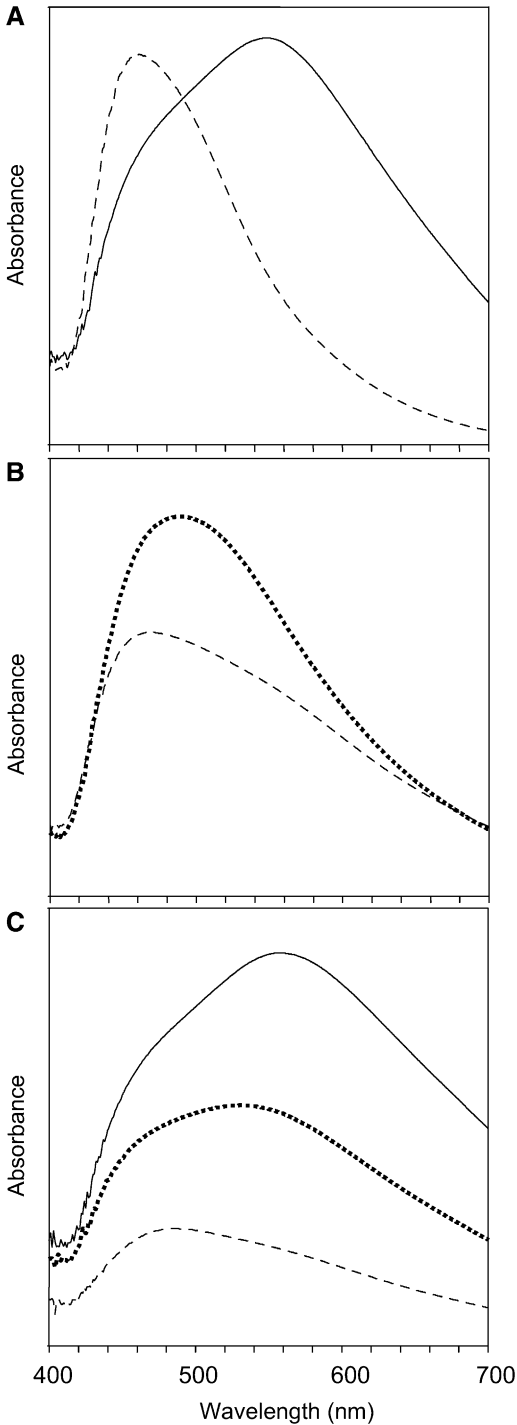


Figure 5. The Absorption Spectra of the Glucans from the Wild Type, the *isa1/isa2* Double Mutant, and the Quadruple DBE Mutant When Complexed with Iodine.

(A) The absorption spectra of potato amylopectin (solid line) and oyster glycogen (dashed line) complexed with iodine. Note that the glycogen concentration was 10 times that of amylopectin.

(B) The absorption spectra of equal amounts of phytyloglycogen from the *isa1/isa2* double mutant (dotted line) and the quadruple DBE mutant

(dashed line) complexed with iodine.

(C) The absorption spectra of equal amounts of starch from the wild type (solid line) and of the insoluble glucans from the *isa1/isa2* double mutant (dotted line) and the quadruple DBE mutant (dashed line) complexed with iodine.

6A). Analysis by high performance anion-exchange chromatography with pulsed amperometric detection (HPAEC-PAD) revealed the presence of maltose and a spectrum of oligosaccharides ranging from approximately d.p. 4 to 17 in size, none of which coeluted with linear malto-oligosaccharide standards (Figure 6B), suggesting that the oligosaccharides were all branched. This was confirmed by pretreatment of the samples with a mixture of *Pseudomonas* isoamylase and *Klebsiella* pululanase, which resulted in glucans that had a smaller average size and coeluted with the linear standards (Figure 6B). The branched oligosaccharides are most likely products of endo-amyolysis by the chloroplastic α -amylase, AMY3 (Yu et al., 2005). Their distribution was bimodal, possibly reflecting the presence of oligosaccharides (d.p. 4 to 10) with one branch point and oligosaccharides (d.p. 9 to 17) with two branch points. Although the total amount of branched oligosaccharides changed only slightly during the day and night (Figure 6A), there were significant fluctuations in the amounts of individual components. Some malto-oligosaccharides were more abundant during the day than at night, whereas other compounds showed the reverse trend (Figure 6C).

Maltose is produced via the exoamyolysis of glucan chains by multiple isoforms of β -amylase (Scheidig et al., 2002; Kaplan and Guy, 2005; Fulton et al., 2008). In the wild type, maltose levels are highest during starch breakdown at night. However, in both *isa1/isa2* and the quadruple mutant, maltose levels were highest during the day (Figure 6A). In *isa1/isa2*, maltose levels increased during the day concomitantly with the accumulation of phytyloglycogen, to levels normally seen in the wild type at night (Delatte et al., 2005). In the quadruple mutant, maltose increased within the first hour of the day to much higher levels than observed in either *isa1/isa2* or the wild type (Figure 6A). These data suggest that β -amylases attack phytyloglycogen during the day. At night, the level of maltose in the quadruple mutant initially remained high but decreased in the second half of the night (Figure 6A), coinciding with the drop in the rate of phytyloglycogen mobilization (Figure 1C).

The degradation of linear chains to release maltose and larger oligosaccharides is consistent with the abundance of very short chains in the glucans of the quadruple DBE mutant. Nevertheless, phytyloglycogen still accumulated gradually during the day (Figure 1C). During the first few hours of the night, around 30% of the phytyloglycogen accumulated in the quadruple mutant was degraded (Figure 1C). We determined the chain length profiles of the methanol-precipitable phytyloglycogen extracted at the end of the day and at different time points during the night. The profiles became progressively enriched in short chains of d.p. 2 to 5 and depleted in chains of d.p. 9 and larger (Figure 7A) after 1, 2, 4, and 8 h of darkness. After 8 h of darkness, the profile did not change further, even when the dark period was extended for 48 h. The

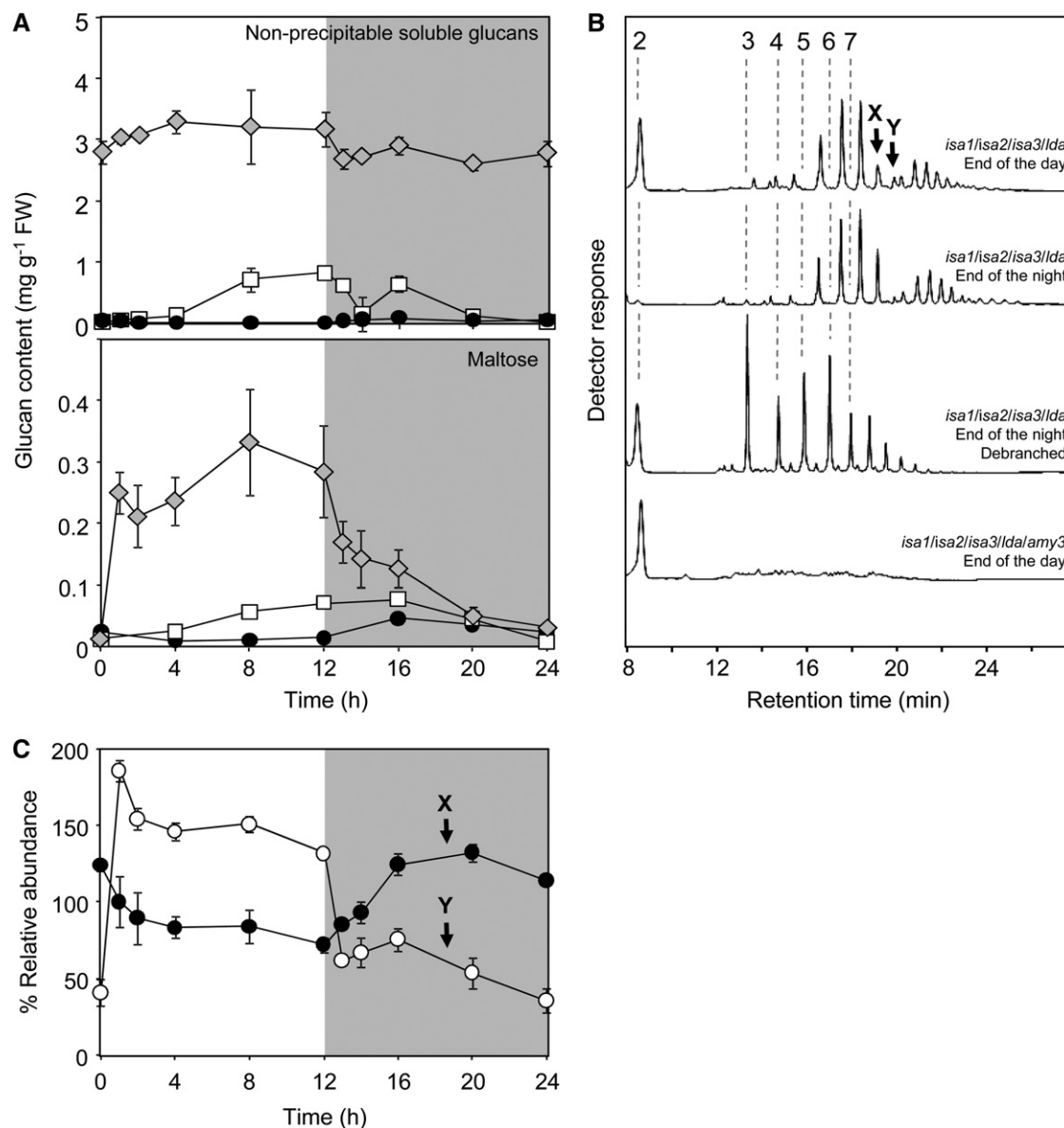


Figure 6. The Quadruple DBE Mutant Contains a Dynamic Pool of Soluble Malto-Oligosaccharides.

(A) Soluble malto-oligosaccharides (top panel) in wild-type (black circles), *isa1/isa2* double mutant (white squares), and quadruple DBE mutant (gray diamonds) plants. Values were calculated by subtracting the methanol-precipitable phytyglycogen from the total pool of soluble glucans. In the quadruple DBE mutant, these glucans comprised maltose and a set of branched oligosaccharides. Maltose (bottom panel) was quantified by HPAEC-PAD.

(B) Representative chromatograms of malto-oligosaccharides present in extracts of the quadruple DBE mutant. Extracts were prepared from plants harvested at the end of the day and at the end of the night, as indicated. Note the difference in maltose content and that the larger oligosaccharides do not elute as linear oligosaccharides (elution times of linear glucans with d.p. 2 to 7 are indicated by dashed lines). Treatment of the end-of-night sample with *Pseudomonas* isoamylase and *Klebsiella* pullulanase results in smaller, linear malto-oligosaccharides and the appearance of maltose, showing that the oligosaccharides were branched. Extracts prepared from the *isa1/isa2/isa3/lda/amy3* quintuple mutant leaves contain maltose but no branched oligosaccharides.

(C) Diurnal changes in the relative peak areas of branched malto-oligosaccharides of d.p. 9 (black circles) and d.p. 10 (white circles), designated X and Y, respectively, in the chromatograms in **(B)**. As standards are not available for these malto-oligosaccharides, the peak areas at each time point were normalized to the average area for that peak over the diurnal cycle. Other peaks in the chromatograms displayed day/night changes in relative abundance, although generally smaller in magnitude.

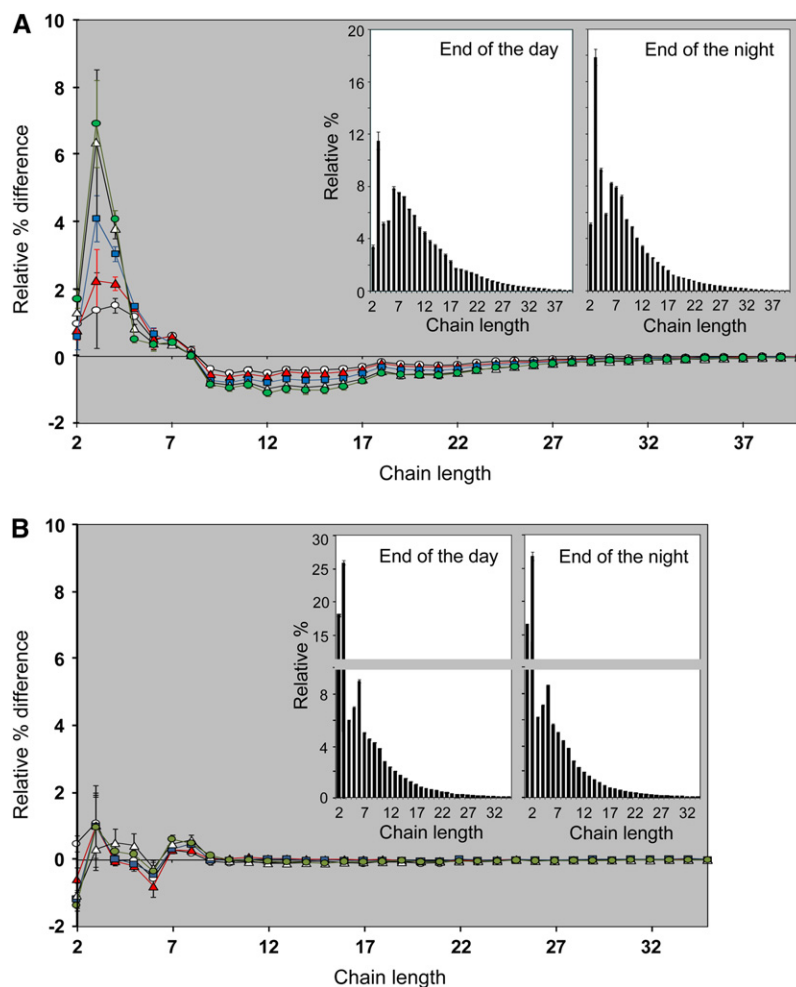


Figure 7. Comparisons of the Chain Length Distributions and the β -Limit Chain Length Distributions of Phytoglycogen from Leaves of the Quadruple DBE Mutant Harvested at Different Times of the Diurnal Cycle.

Phytoglycogen was prepared, debranched, and analyzed as in Figure 2 either without **(A)** or with **(B)** pretreatment with β -amylase. HPAEC-PAD peak areas were summed, and the areas of individual peaks were expressed as percentages of the total. The means \pm SE of three technical replicate digests are shown.

(A) Difference plots derived by subtracting the relative percentage values of the quadruple DBE mutant phytoglycogen extracted at the end of the day from those obtained after 1 h (white circles), 2 h (red triangles), 4 h (blue squares), 8 h (white triangles), and 12 h (green circles) of the night. The SE values of the compared data sets were added together. Note the progressive increase in the relative abundance of short chains during the first 8 h of the night. Chain length distributions of phytoglycogen from the end of the day and the end of the night are shown in the insets.

(B) Difference plots derived by subtracting the relative percentage values of the quadruple DBE mutant β -limit phytoglycogen extracted at the end of the day from those obtained after 1 h (white circles), 2 h (red triangles), 4 h (blue squares), 8 h (white triangles), and 12 h (green circles) of the night. The SE values of the compared data sets were added together. Chain length distributions of β -limit phytoglycogen from the end of the day and the end of the night are shown in the insets. Note the change in the scale of the y axis.

changes in the chain length profile could result from the hydrolysis of external glucan chains until the branch points are reached (i.e., leaving a limit dextrin-like structure that would require debranching for further degradation). To test this, we digested aliquots of the same phytoglycogen samples with an excess of pure β -amylase (from barley endosperm). This enzyme hydrolyzes the external chains of a branched glucan to within two or three glucose residues of a branch point, allowing the determi-

nation of the β -limit (i.e., that remaining after digestion). For amylopectin, the β -limit is typically around 45%, whereas for glycogen, it is 55% (Manners, 1991). The soluble glucan extracted from the quadruple mutant at the end of the day had a β -limit of 56%. At the end of the night, the β -limit had increased to 70%, showing that the outer chains had been preferentially degraded *in vivo* during the night. This conclusion was supported by analyses of the chain length profiles of the β -limit

phytyloglycogens from plants harvested at different time points. All samples had similar profiles, showing that the average internal chain length distribution did not change during the night (Figure 7B).

Loss of AMY3 and All DBEs Increases Glucan Levels and Partially Restores Starch Granule Synthesis

The absence of starch granules in the quadruple mutant supports the idea that DBEs are absolutely required for granule synthesis. However, the metabolism of soluble glucans by hydrolytic enzymes not usually associated with amylopectin synthesis means that this interpretation may be too simple. To investigate this further, the quadruple DBE mutant was crossed with the *amy3* mutant lacking the only chloroplast-localized endoamylase (Yu et al., 2005). The quintuple mutant was selected from the segregating F2 population using PCR to identify plants with homozygous mutations in each gene.

We used HPAEC-PAD to analyze extracts of leaves harvested at the end of the day. This revealed that the pool of small branched oligosaccharides, identified as likely products of α -amylolysis in the quadruple DBE mutant, was absent in the quintuple mutant (Figure 6B). Maltose, however, was still present. Quantitative measurements revealed that the quintuple mutant contained more than twice as much phytoglycogen and 10 times as much insoluble glucan as the quadruple mutant (Figure 8). The insoluble glucan content of the quintuple mutant was comparable to the wild-type level of starch, and the total glucan pool was considerably greater than in the wild type. During the night, the amount of phytoglycogen in the quintuple mutant decreased by around 30%, whereas the amount of insoluble glucan did not change significantly.

The presence of such large amounts of insoluble glucans led us to investigate whether starch granules were present. Iodine staining revealed that the leaves of the quintuple mutant stained much more darkly than the quadruple mutant (see Supplemental Figure 9 online). Using light microscopy, numerous dark-staining particles were observed in the quintuple mutant chloroplasts but were absent from the quadruple DBE mutant chloroplasts (see Supplemental Figure 9 online). In addition, transmission electron microscopy analysis of the quintuple mutant revealed the presence of a diversity of glucan structures and confirmed the presence of well-defined starch granules in all cell types examined (Figure 9). The distribution of glucans was variable and unlike that observed in previously analyzed DBE mutant combinations (Figure 3; see Supplemental Figure 7 online). In the quintuple mutant sections, the same cell types contained glucans with different appearances. For example, some epidermal cells contained many small irregular particles up to 200 nm in diameter, while others in the same section contained starch granules similar in appearance to those found in the wild type. Most palisade cells contained a range of glucans that, in appearance, were most like the glucans in *isa1/isa2* double mutants. However, numerous palisade cell chloroplasts also contained starch granules that ranged from small and irregular to large and smooth.

We analyzed the chain length profiles of the soluble and insoluble glucans in the quintuple mutant. While still quite differ-

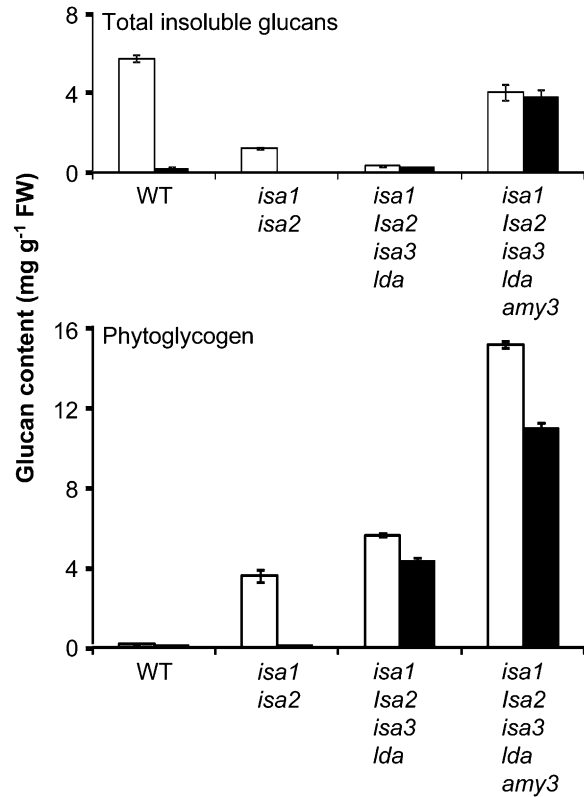


Figure 8. Quantification of Insoluble and Soluble Glucans in the Wild Type, *isa1/isa2*, the Quadruple DBE Mutant, and the Quintuple Mutant Lacking All Four DBEs and the Endoamylase AMY3.

Plants were harvested and immediately frozen in liquid N₂. Each sample comprised a complete individual rosette. Total insoluble and soluble glucans were extracted and measured as in Figure 1. Wild-type and mutant plants were harvested at the end of a 12-h photoperiod (white bars) and at the end of the night (black bars). Each value is the mean \pm SE of four replicate samples. Note the increase in glucan content of the quintuple mutant. A second experiment performed with an independently grown batch of plants yielded similar results.

ent from wild-type amylopectin, the profiles were much less extreme than those of the quadruple mutant (Figure 10). Both the phytoglycogen and insoluble glucan profiles contained fewer short chains (d.p. < 9) and more long chains (d.p. > 9) than the soluble and insoluble glucans from the quadruple mutant. This was particularly apparent for the insoluble glucan fraction. However, it is important to note that the chain length profiles represent the average of all material present in either the phytoglycogen or the insoluble fraction. Thus, there may be insoluble glucans that are closer in structure to the insoluble material in the quadruple DBE mutant and material closer in structure to wild-type starch. This seems likely, considering the range of structures observed by transmission electron microscopy in the quintuple mutant. Collectively, these data show that in the quadruple DBE mutant background, AMY3 activity contributes toward determining the final structure of the glucans

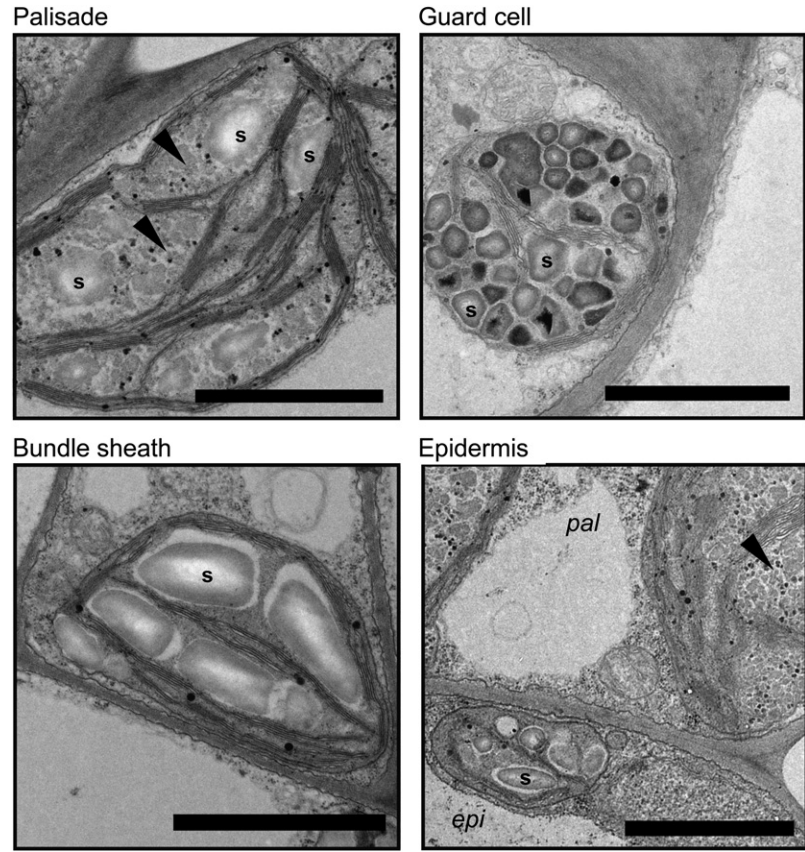


Figure 9. Glucans Accumulating in Plastids of Leaf Cells of the Quintuple Mutant Lacking All Four DBEs and the Endoamylase AMY3, Visualized by Transmission Electron Microscopy.

Starch granules (s) and soluble glucans (black arrowheads) were observed in the plastids of all cell types examined, although there was cell-to-cell variation within the same section. For example, some bundle sheath cells and epidermal cells (epi) appeared to contain only starch granules (shown), whereas others contained soluble glucan or a mixture (not shown). Palisade cell (pal) chloroplasts contained predominantly soluble glucan (most similar in appearance to the material in *isa1/isa2* mesophyll chloroplasts) and infrequent small starch granules. Bars = 2 µm.

synthesized, with the effect of preventing starch granule synthesis and promoting phytyglycogen synthesis.

DISCUSSION

Debranching Is Facilitatory, but Not Mandatory, for Starch Granule Biosynthesis

This study yields important new insight into the biosynthesis of amylopectin and the formation of starch granules. It also highlights one of the major problems in this field of research. As starch is made by the concerted actions of multiple enzymatic activities, removal of one enzyme can alter the substrate of another enzyme and so affect its involvement in the biosynthetic process. Thus, the phenotype resulting from the loss of a single enzyme can really be due to multiple combined effects, each of which is difficult to quantify. For example, the accumulation of maltose at the same time as phytyglycogen in the *isa1/isa2* mutants shows that the loss of the isoamylase creates a sub-

strate for β -amylase, which in turn affects glucan structure (Figure 6) (Delatte et al., 2005). These combined effects become much more complex when (1) two or more proteins are removed, (2) protein-protein interactions between biosynthetic enzymes are considered (Tetlow et al., 2004, 2008; Hennen-Bierwagen et al., 2008), or (3) plastidial enzymes not normally participating in amylopectin biosynthesis act on aberrant glucans to influence the final glucan structure (as in this study). Unless such enzymatic interdependencies are disentangled, misinterpretations of mutant phenotypes are likely.

Our comprehensive analysis of all of the combinations of DBE mutants revealed that the different isoforms have different roles in starch metabolism and that no starch granules are synthesized when all DBEs are missing. Although these data appear to support the idea that DBEs play an essential role in granule formation, we argue that our additional results disprove this hypothesis. By mutating *AMY3* in addition to the DBEs, we have shown that starch granules can be synthesized without DBEs. The structure of the amylopectin in the quintuple mutant is not reverted back to that of the wild type and phytyglycogen still

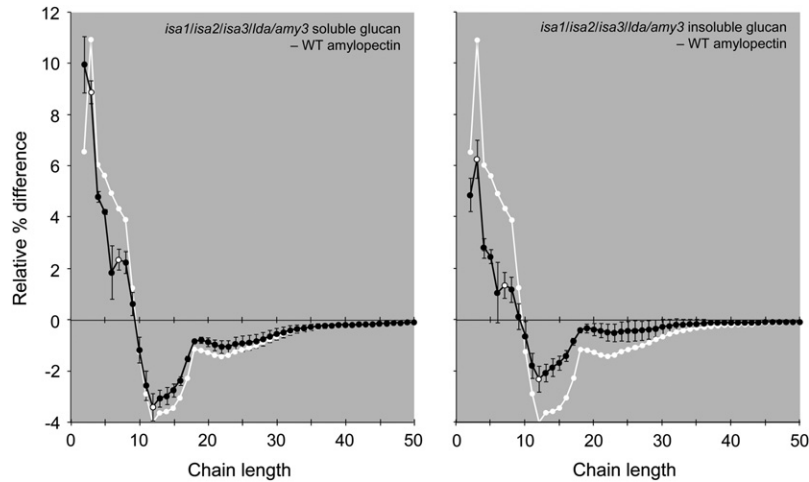


Figure 10. Changes in the Chain Length Distributions of Glucans Extracted from Leaves of the Quintuple Mutant Lacking All Four DBEs and the Endoamylase AMY3.

Phytoglycogen and insoluble glucans were prepared and analyzed as in Figure 2. Peak areas were summed, and the areas of individual peaks were calculated as a percentage of the total \pm SE of three technical replicates. The difference plots shown were derived by subtracting the relative percentage values of wild-type amylopectin from the quintuple mutant glucans. Open symbols are placed at d.p. 3, 7, and 12. The SE values of the compared data sets were added together. For ease of comparison, the difference plot of phytoglycogen from the quadruple DBE mutant (grown alongside the quintuple mutant, without SE values) is shown in white.

accumulates. Nevertheless, the coordinated actions of isoforms of starch synthase and branching enzyme appear to have sufficient substrate specificity to synthesize an amylopectin-like polymer capable of crystallization. However, we emphasize in our model (below) that debranching is likely to be part of the normal amylopectin biosynthetic pathway in wild-type plants.

The Function of ISA1 and ISA2

The multimeric ISA1-containing isoamylase has an important role in facilitating amylopectin biosynthesis (James et al., 1995; Mouille et al., 1996; Nakamura et al., 1997; Burton et al., 2002; Posewitz et al., 2004; Delatte et al., 2005; Wattedled et al., 2005). Our analyses of the single and multiple mutants in which *ISA1* and/or *ISA2* are mutated alone or in combination with the remaining DBE genes support the idea that *ISA1* and *ISA2* proteins work exclusively together as a multimeric holoenzyme in *Arabidopsis*. In each case, mutation of *ISA1*, *ISA2*, or both has the same effect. However, in rice and possibly the other cereals, *ISA1* occurs both as a homomultimer and as a heteromultimer with *ISA2* (Utsumi and Nakamura, 2006), and the impact of mutating *ISA2* in these species has yet to be established.

All *isa1* mutants accumulate phytoglycogen, but there is variation in the degree to which this occurs. In cereal endosperms and *Arabidopsis* leaves, residual starch granules are still synthesized, sometimes in a tissue-specific or cell type-specific pattern, and often containing amylopectin with an altered structure compared with the respective wild type (Nakamura et al., 1997; Dinges et al., 2001; Burton et al., 2002; Wong et al., 2003; Delatte et al., 2005; Wattedled et al., 2005). In *Chlamydomonas*, total glucan accumulation is reduced to <8% of the wild type,

and most of this is phytoglycogen (<3% compared with the wild type is found in the insoluble fraction) (Mouille et al., 1996; Posewitz et al., 2004). These phenotypic variations have shown that *ISA1* is not essential for starch granule biosynthesis but left open the possibility that *ISA3* and/or *LDA* may substitute for *ISA1*. While our results show that *ISA3* and *LDA* can facilitate starch granule synthesis in the absence of *ISA1*, they also indicate that the different DBEs have distinct specificities *in vivo*. For example, loss of *ISA3* does not result in the same glucan structural changes as the loss of *ISA1/ISA2*. In the triple isoamylase mutant, the phenotypes of *isa3* and *isa1/isa2* are merged (Figure 2). This indicates that *ISA3* removes different branches than *ISA1/ISA2*. These conclusions are consistent with the analysis of activities of recombinant and purified isoamylases (Hussain et al., 2003; Takashima et al., 2007). Therefore, when *ISA3* does serve to promote starch granule formation, it probably does so in a different way than *ISA1/ISA2*.

Delatte et al. (2005) suggested that the *ISA1/ISA2* complex may remove branch points located too close to other branch points. Modeling studies have suggested that very short or very long interbranch distances would inhibit the optimal alignment of double helices and therefore the formation of semicrystalline lamellae (O'Sullivan and Perez, 1999). According to this idea, it is plausible that the alteration in structure resulting from the loss of *ISA1/ISA2* retards the crystallization of amylopectin without preventing it altogether. Delayed crystallization would render nascent glucans susceptible to further modification. The concomitant accumulation of maltose with phytoglycogen in *isa1* and *isa2* mutants (Delatte et al., 2005) suggests that β -amylase attacks the nascent glucans. By contrast, maltose levels in the wild type remain low during the day as starch accumulates (Chia

et al., 2004; Lu and Sharkey, 2004; Niittylä et al., 2004; Fulton et al., 2008), implying less β -amylolysis than in *isa1/isa2* mutants. In this study, we have also shown that the products of α -amylase accumulate when all DBEs are missing. It seems likely that α -amylase also attacks the glucans synthesized in *isa1/isa2* mutants, but its products do not accumulate in the stroma, presumably due to the presence of ISA3 and LDA. Thus, the view that loss of ISA1 is the sole cause of phytoglycogen accumulation may be incorrect, and α - and β -amylases may significantly influence glucan structure and solubility. Interestingly, the presence of malto-oligosaccharides alongside phytoglycogen has also been reported for the *isa1* mutant of *Chlamydomonas* (*sta7*; Mouille et al., 1996).

We suggest that the major function of the ISA1/ISA2 isoamylase is to accelerate the crystallization of nascent amylopectin molecules and thereby prevent the interference of enzymes such as amylases in the biosynthetic process. Indeed, recent discoveries suggest that, once crystalline, amylopectin is resistant to degradation and requires disruption via glucan phosphorylation before it can be effectively degraded (Edner et al., 2007; Zeeman et al., 2007; Hejazi et al., 2008).

The Functions of ISA3 and LDA

Previous analyses have suggested that the roles of LDA and ISA3 in vivo are primarily in the breakdown of starch (Wattebled et al., 2005; Delatte et al., 2006). It is known that LDA and ISA3 preferentially remove short branches and have their highest activity on β -limit dextrans (Wu et al., 2002; Hussain et al., 2003; Delatte et al., 2006; Takashima et al., 2007). However, branching enzymes do not generate branches as short as d.p. 3 (Borovsky et al., 1975; Guan and Preiss, 1993; Takeda et al., 1993), suggesting that the preferred substrates of LDA and ISA3 are produced by the activities of other glucan-catabolizing enzymes that shorten chains (i.e., α - and β -amylases).

Here, we have shown that both ISA3 and LDA can influence the structure of glucans, although there appears to be considerable functional overlap between the two enzymes. A role in facilitating starch granule biosynthesis is only revealed when all of the other DBEs are already missing. The severe phenotype of the quadruple DBE mutant relative to *isa1/isa2/isa3* and *isa1/isa2/lda* shows that either ISA3 or LDA activity is sufficient to promote the formation of some starch granules in the *isa1/isa2* background. However, the restoration of starch granule synthesis upon removal of AMY3 from the quadruple DBE mutant suggests that this is not because debranching per se is required. The evidence that amylases degrade glucans synthesized in the absence of ISA1/ISA2 allows us to propose an explanation for the conditional involvement of ISA3 and LDA. We envisage that continual amylolytic turnover generates very short chains, which restricts the formation and subsequent packing of double helices. Removal of such very short chains by ISA3 and/or LDA, therefore, could serve to promote crystallization and thus granule formation. The increase in the number of very short chains in the *isa1/isa2/isa3* triple mutant compared with *isa1/isa2* is consistent with this idea and shows that very short branches are being actively removed by ISA3 in *isa1/isa2* during periods of net glucan accumulation (Figure 2). The fact that no such change in struc-

ture is seen in the *isa1/isa2/lda* triple mutant, relative to *isa1/isa2*, indicates that ISA3 is able to fully compensate for the loss of LDA, as is the case during starch breakdown (Delatte et al., 2006).

A Model Explaining the Mutant Phenotypes and DBE Function in Amylopectin Biosynthesis

Collectively, the phenotypic data and the existing knowledge of the substrate preferences of the different enzymes allow us to propose schemes of glucan metabolism in the different mutant combinations and explain if and when each DBE acts during amylopectin biosynthesis (Figure 11). In our model, the removal of misplaced branch points by ISA1/ISA2 is a normal part of the starch biosynthetic process. This ensures rapid formation of semicrystalline lamellae, which are not susceptible to further modification. Thus, amylases do not have access to the nascent glucans and do not participate in biosynthesis. When ISA1/ISA2 is missing, crystallization is still possible, but inefficient. This exposes the nascent glucans to modification by other enzymes, including α - and β -amylases, which generate short chains that prevent crystallization. Removal of short chains by ISA3 or LDA promotes crystallization, explaining the residual starch granules in *isa1/isa2* and its absence in the quadruple DBE mutant. Removal of AMY3 decreases the extent of the modifications of nascent glucans, allowing some crystallization to occur independently of debranching. The presence of β -amylases in the quintuple mutant explains why the structure of the glucans is still rich in short chains and why a significant fraction of the glucan still occurs as phytoglycogen. We predict that further removal of β -amylases will result in a structure closer to that produced by the starch synthases and branching enzymes and that an even greater fraction will occur as starch granules.

One possible discrepancy in our model is the fact that the amylopectin structure of *isa3* single mutants is slightly enriched in very short chains, although no phytoglycogen is produced. This could mean that a small amount of chain degradation occurs even in the presence of ISA1/ISA2. However, Delatte et al. (2006) concluded that the very short chains of the *isa3* mutant amylopectin arose during incomplete breakdown of starch at night and became buried within the granules as starch accumulated to high levels. Further work will be required to distinguish between these possibilities.

An increased susceptibility of nascent amylopectin molecules to amylolytic attack might also help to explain the increase in the number of starch granules frequently observed in isoamylase mutants (Figure 3; see Supplemental Figure 7 online) (Burton et al., 2002; Bustos et al., 2004). Branched oligosaccharides could potentially serve as nucleation sites for new starch granules. In the absence of DBEs, such oligosaccharides may be metabolized less efficiently, as suggested previously (Burton et al., 2002; Bustos et al., 2004), but may also be produced more readily by endoamylolysis.

It is not clear why some cell types are more prone to accumulating phytoglycogen than others (Figures 3 and 9; see Supplemental Figure 7 online) (Delatte et al., 2005). Cell type-specific expression of genes encoding glucan-synthesizing enzymes (starch synthases, branching enzymes, ISA1 and ISA2) seems the most likely explanation. However, this study emphasizes that

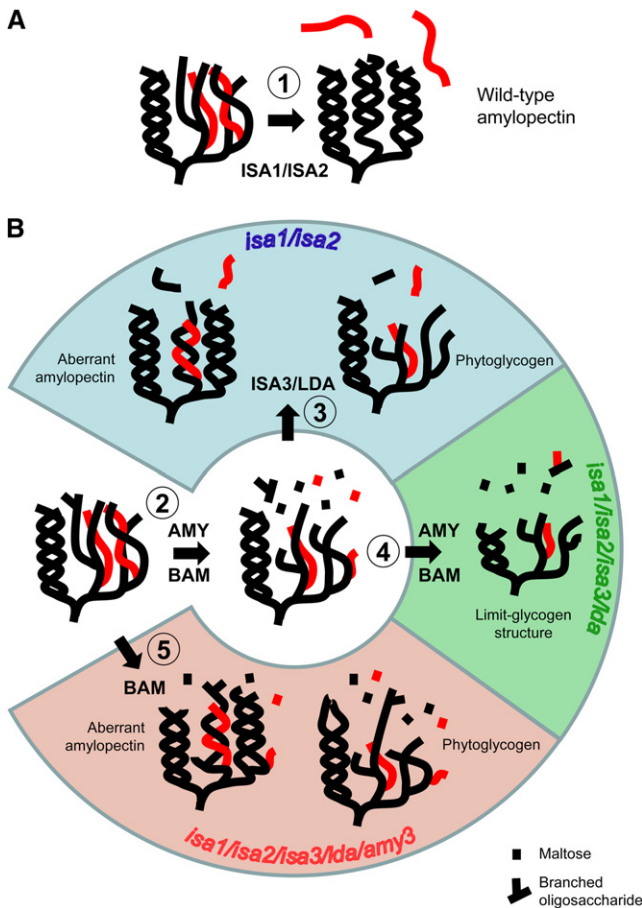


Figure 11. Models of Amylopectin Synthesis in the Wild Type and Aberrant Glucan Synthesis in the Mutant Combinations Studied Here.

(A) Glucans produced by starch synthases and starch branching enzymes produce a branched amylopectin-like glucan capable of crystallization to form starch granules. This process is accelerated by the ISA1/ISA2 heteromultimeric enzyme (1), which selectively removes wrongly positioned branch points (red).

(B) Glucans produced by starch synthases and starch branching enzymes, as in (A), are not selectively debranched in the absence of ISA1 and/or ISA2, delaying the formation of secondary structures and rendering the glucans susceptible to α - and β -amylolysis. This results in the formation of short chains and liberation of maltose and branched malto-oligosaccharides (2). In the *isa1/isa2* double mutant, very short chains can still be removed by ISA3 and/or LDA, enabling some aberrant amylopectin to be synthesized, but the majority of glucans remain soluble as phytoglycogen (3; blue section). Differences in amylolytic capacity may explain why some cells preferentially make starch granules (e.g., epidermal cells) and others make phytoglycogen (mesophyll cells). In the absence of all DBEs, the aberrant glucans cannot be degraded and are susceptible to further amylolysis, resulting in a limit glycogen-like structure (4; green section). In the absence of all DBEs and AMY3, nascent amylopectin produced by starch synthases and starch branching enzymes are subjected to β -amylolysis but not α -amylolysis (5; red section). Reduced amylolytic modification of the glucan allows a greater fraction to crystallize. We predict that removal of BAM proteins would further favor starch granule production. We emphasize that these schemes are simplified and that rather than being a linear or discontin-

a wider set of genes must be taken into account (e.g., *ISA3*, *LDA*, α - and β - amylases, and disproportionating enzyme). Therefore, we consider it unlikely that DBE expression patterns alone could explain such drastic local phenotypic differences.

Nanoscale Particles in Plants Lacking All DBEs

Given the abundance of short chains in the glucans in the quadruple DBE mutant, it is surprising that some still form insoluble, nanometer-scale spherical particles. The λ_{max} of this material when complexed with iodine is similar to that of the soluble phytoglycogen that is synthesized simultaneously and more reminiscent of a glycogen-like polymer than of amylopectin. Most chains are too short to form the secondary and tertiary structures that are typically associated with amylopectin and that confer the insoluble property of starch. Earlier studies with ISA1-deficient maize also documented that, in addition to starch granules, glucan with glycogen-like properties could be sedimented by relatively gentle centrifugation (Matheson, 1975; Boyer et al., 1981), consistent with the fact that tiny particles could also be isolated from the *isa1/isa2* double mutants (Figure 4). Furthermore, glycogen-like granules have been isolated from the cyanobacterium *Nostoc muscorum* (Chao and Bowen, 1971). It is not clear what features of these particles render them insoluble, although several possibilities exist. The particles may contain an insoluble core representing the sites of starch granule initiation. Elaboration of this core with noncrystalline material may result in the spherical particles observed. However, the mechanism of granule initiation is not yet well understood (Roldán et al., 2007), and the insoluble particles do not contain significant amounts of protein. Alternatively, secondary structures distinct from those of amylopectin may occur in a stochastic way and result in some insoluble particles in a background of soluble glucan. Further analysis of these glucans will be required to evaluate fully their properties, although the low levels present in the *Arabidopsis* quadruple DBE mutant make this a challenging task.

Loss of All DBEs Prevents Glucan Degradation

A distinct feature of the quadruple DBE mutant is its inability to mobilize all of its glucans in the dark. During the night, there is a 30% decrease in the amount of glucan in the leaf due to rapid mobilization during the initial few hours of the night. Collectively, our data suggest that a pool of phytoglycogen with very short external chains is formed that cannot be further degraded without debranching. First, while the number of very short chains in the phytoglycogen increases progressively during the first 8 h of the night, the chain length distribution of the β -limit glucan remains essentially unaltered. This shows that the degradation primarily affects only the exposed outer chains. The extent to which the extracted phytoglycogen could be degraded *in vitro* by

uous process, as indicated, the glucans are likely to be continuously elaborated and degraded during synthesis. However, we propose that the schemes serve as a good basis for further evaluation.

an excess of barley β -amylase decreased between the end of the day and the end of the night (44 and 30% was degraded, respectively). Given that β -amylases play a key role in starch degradation (Scheidig et al., 2002; Kaplan and Guy, 2005; Fulton et al., 2008), it is not clear why the phytoglycogen is not degraded to the same extent in vivo. However, the exact β -limit will depend on the properties of the β -amylase isoforms present in the chloroplast (Fulton et al., 2008). Second, the quadruple mutant contains a pool of small branched malto-oligosaccharides resulting from endoamylolysis by AMY3. Although the marked increase in total glucan content in the quintuple mutant illustrates that AMY3 does contribute to the glucan degradation observed in the quadruple DBE mutant, it is unclear what prevents AMY3 from completely degrading all of the phytoglycogen to branched malto-oligosaccharides. Possible explanations include inhibition of AMY3 by its accumulated products or that AMY3 is unsuited to degrade hyperbranched β -limit glycogen (e.g., due to steric hindrances).

In summary, this study represents an important step toward understanding the minimal set of enzymes required for starch synthesis. While DBEs participate, they are not essential in *Arabidopsis*, as starch granules can be made even when all DBEs are missing (by removing another amyolytic activity). Given the extent of conservation in the starch biosynthetic genes, DBEs specifically (Rahman et al., 2003), in both higher plants and green algae, these conclusions from *Arabidopsis* are likely to have broad significance. In other systems in which DBE function has been studied (such as cereal endosperms and *Chlamydomonas* cells), a similar situation may occur, as native gel analyses have revealed that multiple amyolytic activities are present in such tissues in addition to DBEs (Mouille et al., 1996; Nakamura et al., 1997; Dinges et al., 2001; Burton et al., 2002). Furthermore, this study shows that DBEs are essential for the subsequent breakdown of the glucans synthesized by starch synthases and branching enzymes.

METHODS

Plant Material and Growth Conditions

Arabidopsis thaliana plants (ecotype Columbia) were grown in a nutrient-rich, medium-grade, peat-based compost in a Percival AR95 growth chamber (CLF Plant Climatics) at a constant temperature of 20°C, 70% RH, with a 12-h photoperiod. The light intensity was uniform at 150 $\mu\text{mol quanta}\cdot\text{m}^{-2}\cdot\text{s}^{-1}$. Seeds were sown by hand. After seedling establishment, individuals were pricked out into 200-mL pots. Details of the DBE mutants used in this study, including references describing their initial characterization, are presented in Supplemental Table 1 online. The mutations in *ISA1*, *ISA3*, and *LDA* result from T-DNA insertions. The mutation in *ISA2* is a single base pair deletion, for which we developed a cleaved-amplified polymorphic sequence marker. All mutants are in the Columbia background. Lines carrying multiple mutations were obtained by crossing and selecting homozygous plants of the required genotypes from the segregating F2 populations using PCR-based and cleaved-amplified polymorphic sequence-based genotyping. Primer sequences for DBE genes are given in Supplemental Table 1 online. The primers used for the identification of the *amy3-2* allele (SAIL_613D12; Yu et al., 2005) were as follows: T-DNA-specific primer, 5'-GCCTTTTCAGAAATGGA-TAAATAGCCTTGCTTCC-3'; AMY3-specific primers, 5'-CCGACCTTGT-GAAATTTCTTCACTG-3' and 5'-GGTTCCTCTGTAGACGATGTTCC-3'.

Extraction and Analysis of Enzymatic Activity by Native PAGE

Native polyacrylamide gels for the detection of starch-hydrolyzing enzymes were used as described by Zeeman et al. (1998a), and those for the detection of starch synthases and branching enzymes were used as described by Nishi et al. (2001).

Extraction and Measurement of Metabolites

Samples (300 to 600 mg fresh weight) comprising all of the leaves or the entire rosette of an individual plant (30 to 35 d old, depending on the genotype) were harvested, frozen in liquid N_2 , and subsequently extracted in 2 to 4 mL (depending on sample weight) of ice-cold 1 M perchloric acid using an all-glass homogenizer as described by Delatte et al. (2005). Insoluble material was washed once with water to remove residual soluble glucans and three times with 80% (v/v) ethanol. Glucans in the insoluble fraction (including starch granules) and in the soluble fraction (including phytoglycogen and malto-oligosaccharides) were determined by measuring the amount of glucose released by treatment with α -amylase and amyloglucosidase (Smith and Zeeman, 2006). Phytoglycogen was precipitated by the addition of three volumes of methanol and collected by centrifugation (3000g). Low molecular weight malto-oligosaccharides in the soluble fraction that were not precipitated by methanol were analyzed using HPAEC-PAD. Samples were evaporated to dryness, redissolved in water (100 μL), and then applied to sequential 1.5-mL columns of Dowex 50W and Dowex 1 (Sigma-Aldrich). The neutral compounds were eluted with 4 mL of water, lyophilized, and redissolved in 100 μL of water. Malto-oligosaccharides were separated on a Dionex PA-200 column according to the following conditions: eluent A, 100 mM NaOH; eluent B, 150 mM NaOH and 500 mM sodium acetate. The gradient was as follows: 0 to 7 min, 100% A; 7 to 20 min, a linear gradient to 60% A and 40% B (maltose elution); 20 to 35 min, a linear gradient to 45% A and 55% B (malto-oligosaccharide elution); 35 to 45 min, a linear gradient to 15% A and 85% B (column wash step); 45 to 60 min, step to 100% A (column reequilibration). The flow rate was 0.5 mL/min. Peaks were identified by coelution with malto-oligosaccharide standards. Peak areas were determined using Chromeleon software.

Structural Analysis of Glucans

For iodine staining, plants were harvested at the end of a 12-h photoperiod, decolorized with hot ethanol, and stained for starch with Lugol solution. Mesophyll cells were viewed by light microscopy using an Olympus BX3 microscope with CellR imaging software. The λ_{max} of purified glucans was determined by mixing 50 to 100 μg of glucan with 10% (v/v) Lugol solution and scanning the absorbance between the wavelengths of 400 and 700 nm.

Soluble and insoluble fractions from the perchloric acid-extracted material used for the measurement of phytoglycogen and insoluble glucans (above) were also used for glucan structural analysis. Equal quantities of glucan from four or more individually extracted plants were pooled to yield sufficient material for chain length analyses. Glucan samples (50 to 100 μg) were boiled for 15 min in water. After treatment with *Pseudomonas* isoamylase (Sigma-Aldrich) and *Klebsiella* pullulanase (Megazyme) to debranch glucans (1 unit of each enzyme for 2 h at 37°C in 10 mM Na-acetate, pH 4.8), samples were passed through sequential Dowex 50 and Dowex 1 minicolumns (as above) to remove contaminating proteins and charged compounds. The neutral glucan chains were eluted with four column volumes of water, lyophilized, and redissolved in 100 μL of water. HPAEC-PAD analysis of the linear chains was performed using a Dionex PA-200 column using the following gradient: 0 to 13 min, a linear gradient from 95% A and 5% B to 60% A and 40% B; 13 to 50 min, a linear gradient to 15% A and 85% B (linear

chain elution); 50 to 70 min, step to 95% A and 5% B (column reequilibration). The flow rate was 0.5 mL/min.

β -Limit glucans were prepared by incubating glucan samples (50 or 100 μ g) with 100 units of barley endosperm β -amylase (Megazyme) for 2 h at 37°C in 10 mM MES, pH 6.5, and 1 mM DTT. The β -limit glucans were precipitated by the addition of 3 volumes of methanol, collected by centrifugation (3000g), and then redissolved in water. Subsequent debranching, sample treatment, and HPAEC-PAD analyses were performed as described above.

Purification of Starch Granules and Other Insoluble Glucans

Plants (50 g fresh weight) were harvested at the end of the light period, frozen in liquid N₂, and extracted using a Waring blender in 250 mL of ice-cold medium containing 0.1 M Na-acetate (pH 4.8), 0.05% Triton X-100, and 2 mM EDTA. The homogenate was filtered through Miracloth, and SDS was added to a final concentration of 1.5% (w/v). The material, including starch granules and/or other insoluble glucans, was pelleted by centrifugation at 20,000g for 20 min. The pellet was washed five times with water to remove residual SDS. Cell debris was removed by sequential filtration through nylon meshes with 100-, 22-, and 6- μ m pore sizes. The resultant insoluble material was washed another four times in water.

Electron Microscopy

Procedures for transmission electron microscopy were as described by Delatte et al. (2005) except that leaf samples were fixed in 2% glutaraldehyde in 0.1 M sodium cacodylate buffer, pH 7.4, for 4 h at 4°C. Tissue was washed six times in cold 0.1 M sodium cacodylate buffer, pH 7.4, postfixed overnight in 1% (w/v) aqueous osmium tetroxide, 0.1 M sodium cacodylate buffer, pH 7.4, at 4°C, and then washed another six times in cold 0.1 M sodium cacodylate buffer, pH 7.4, and once with water. Then, sections were dehydrated in an ethanol series and infiltrated and embedded in epoxy resin (Spurr's; Agar Scientific). Ultrathin sections were cut with a diamond knife and stained sequentially with uranyl acetate and Reynold's lead citrate. Stained sections were examined using a Phillips BioTwin CM100 or a FEI Morgagni 268 electron microscope.

For cryoscanning electron microscopy, carbon films (8 nm) mounted on copper grids (400 mesh/inch) were used as support. Prior to adsorption, the support films were rendered hydrophilic (glow discharged) in a Harrick Plasma cleaner. Samples were adsorbed for 1 min to the support by placing it upside down onto a 3- μ L sample drop. Excess water was removed, and the grids were frozen by dipping into liquid nitrogen. While submersed, grids were mounted on a cryostage and the specimen surface was covered with a cold copper shield to trap environmental water during the transfer to the high-vacuum chamber of a freeze-etching device (BAF060; Bal-Tec). Samples were freeze-dried by increasing the temperature to -80°C for 20 min under high vacuum (Wepf et al., 1991) and then unidirectionally shadowed with tungsten. Transfer to the electron microscope was done under high-vacuum conditions at -140°C (VCT010; Bal-Tec) (Richter et al., 2007) to prevent the recrystallization of inherent water and recontamination. Imaging was performed with a field emission scanning electron microscope (Leo Gemini 1530; Carl Zeiss) equipped with a cold stage.

FTIR Spectroscopy

FTIR spectra of insoluble glucans purified from different mutants were recorded in the reflectance mode using a Perkin-Elmer spectrophotometer (Spectrum One). Glucans were suspended in water to a final concentration of 10 μ g/ μ L. Twenty microliters of the suspension was applied to the ATR diamond crystal and air-dried. The spectra were collected from 4000 to 600 cm⁻¹ at a resolution of 4 cm⁻¹. Spectra were recorded against an empty cell as background and baseline-corrected.

Accession Numbers

Arabidopsis Genome Initiative gene codes for the *Arabidopsis* genes discussed in this study are as follows: ISA1, At2g39930; ISA2, At1g03310; ISA3, At4g09020; LDA, At5g04360; AMY3, At1g69830. Further information, including line identifiers for the DBE mutants obtained from the SALK and GABI_KAT collections, is provided in Supplemental Table 1 online.

Supplemental Data

The following materials are available in the online version of this article.

Supplemental Figure 1. A Model of Amylopectin Structure.

Supplemental Figure 2. Analysis of Glucan-Metabolizing Enzymes Using Native PAGE.

Supplemental Figure 3. Comparison of the Glucan Contents of *isa1/lda* and *isa2/lda* Double Mutants with the Respective *isa* Single Mutants.

Supplemental Figure 4. Comparisons of the Chain Length Distributions of Glucans Extracted from Leaves of the *isa1/isa2* Double Mutant and the *isa1/isa2/lda* Triple Mutant.

Supplemental Figure 5. Comparisons of the Chain Length Distributions of Glucans Extracted from Leaves of the *isa1* and *isa2* Single Mutants and the *isa1/lda* and *isa2/lda* Double Mutants.

Supplemental Figure 6. Equivalence between the Chain Length Distributions of the Glucans within the Mutant Groups *isa1/isa3*, *isa2/isa3*, *isa1/isa2/isa3* and *isa1/isa3/lda*, *isa2/isa3/lda*, *isa1/isa2/isa3/lda*.

Supplemental Figure 7. Visualization of the Glucans Accumulating in Plastids of Different Cell Types of Wild-Type and DBE Mutant Plants Using Transmission Electron Microscopy.

Supplemental Figure 8. FTIR Spectra of Wild-Type Starch and the Insoluble Glucans from *isa1/isa2* and the Quadruple DBE Mutant.

Supplemental Figure 9. Iodine Staining of Wild-Type, *isa1/isa2/isa3/lda* Quadruple Mutant, and *isa1/isa2/isa3/lda/amy3* Quintuple Mutant Plants.

ACKNOWLEDGMENTS

We thank Martine Trevisan for technical assistance, Roger Wepf, Peter Wägli, Heinz Gross, and Liliane Diener for assistance with electron microscopy, Sabine Klarer for assistance with plant growth, Christina Streb for assistance with FTIR spectroscopy, and Maria Henriksson and Alison Smith for critical review of the manuscript. The work was funded by the Swiss National Science Foundation (Grant 3100AO-116434/1) and the Roche Research Foundation.

REFERENCES

Ball, S., Guan, H.-P., James, M., Myers, A., Keeling, P., Mouille, G., Buléon, A., Colonna, P., and Preiss, J. (1996). From glycogen to amylopectin: A model for the biogenesis of the plant starch granule. *Cell* **86**: 349–352.

- Borovsky, D., Smith, E.E., and Whelan, W.J.** (1975). Purification and properties of potato 1,4- α -D-glucan-1,4- α -D-glucan 6- α -(1,4- α -glucano)-transferase: Evidence against a dual catalytic function in amylose-branching enzyme. *Eur. J. Biochem.* **59**: 615–625.
- Boyer, C. D., Damewood, P. A. and Simpson, E. K. G.** (1981). The possible relationship of starch and phytoglycogen in sweet corn. I. Characterisation of particulate and soluble polysaccharides. *Starch/Stärke* **33**: 125–130.
- Bradford, M.M.** (1976). A rapid and sensitive method for the quantitation of micrograms quantities of protein utilizing the principle of protein-dye binding. *Anal. Biochem.* **72**: 248–254.
- Buléon, A., Colonna, P., Planchot, V., and Ball, S.** (1998). Starch granules: Structure and biosynthesis. *Int. J. Biol. Macromol.* **23**: 85–112.
- Burton, R.A., Jenner, H., Carrangis, L., Fahy, B., Fincher, G.B., Hylton, C., Laurie, D.A., Parker, M., Waite, D., van Wegen, S., Verhoeven, T., and Denyer, K.** (2002). Starch granule initiation and growth are altered in barley mutants that lack isoamylase activity. *Plant J.* **31**: 97–112.
- Bustos, R., Fahy, B., Hylton, C.M., Seale, R., Nebane, N.M., Edwards, A., Martin, C., and Smith, A.M.** (2004). Starch granule initiation is controlled by a heteromultimeric isoamylase in potato tubers. *Proc. Natl. Acad. Sci. USA* **101**: 2215–2220.
- Capron, I., Robert, P., Colonna, P., Brogly, M., and Planchot, V.** (2007). Starch in rubbery and glassy states by FTIR spectroscopy. *Carbohydrate Polymers* **68**: 249–259.
- Chao, L., and Bowen, C.C.** (1971). Purification and properties of glycogen isolated from a blue-green alga, *Nostoc muscorum*. *J. Bacteriol.* **105**: 331–338.
- Chia, T., Thorneycroft, D., Chapple, A., Messerli, G., Chen, J., Zeeman, S.C., Smith, S.M., and Smith, A.M.** (2004). A cytosolic glucosyltransferase is required for conversion of starch to sucrose in *Arabidopsis* leaves at night. *Plant J.* **37**: 853–863.
- Dauvillée, D., Colleoni, C., Mouille, G., Morell, M.K., d’Hulst, C., Wattebled, F., Liénard, L., Delvallé, D., Ral, J.-P., Myers, A.M., and Ball, S.G.** (2001). Biochemical characterisation of wild-type and mutant isoamylases of *Chlamydomonas reinhardtii* supports a function of the multimeric enzyme organisation in amylopectin maturation. *Plant Physiol.* **125**: 1723–1731.
- Delatte, T., Trevisan, M., Parker, M.L., and Zeeman, S.C.** (2005). *Arabidopsis* mutants *Atisa1* and *Atisa2* have identical phenotypes and lack the same multimeric isoamylase, which influences the branch point distribution of amylopectin during starch synthesis. *Plant J.* **41**: 815–830.
- Delatte, T., Umhang, M., Trevisan, M., Eicke, S., Thorneycroft, D., Smith, S.M., and Zeeman, S.C.** (2006). Evidence for distinct mechanisms of starch granule breakdown in plants. *J. Biol. Chem.* **281**: 12050–12059.
- Dinges, J.R., Colleoni, C., James, M.G., and Myers, A.M.** (2003). Mutational analysis of the pullulanase-type debranching enzyme of maize indicates multiple functions in starch metabolism. *Plant Cell* **15**: 666–680.
- Dinges, J.R., Colleoni, C., Myers, A.M., and James, M.G.** (2001). Molecular structure of three mutations at the maize *sugary1* locus and their allele-specific phenotypic effects. *Plant Physiol.* **125**: 1406–1418.
- Edner, C., Li, J., Albrecht, T., Mahlow, S., Hejazi, M., Hussain, H., Kaplan, F., Guy, C., Smith, S.M., Steup, M., and Ritte, G.** (2007). Glucan, water dikinase activity stimulates breakdown of starch granules by plastidial beta-amylases. *Plant Physiol.* **145**: 17–28.
- Fujita, N., Kubo, A., Francisco, P.B., Nakakita, M., Harada, K., Minaka, N., and Nakamura, Y.** (1999). Purification, characterisation and cDNA structure of isoamylase from developing endosperm of rice. *Planta* **208**: 283–293.
- Fulton, D.C., et al.** (2008). β -AMYLASE4, a noncatalytic protein required for starch breakdown, acts upstream of three active β -amylases in *Arabidopsis* chloroplasts. *Plant Cell* **20**: 1040–1058.
- Guan, H.P., and Preiss, J.** (1993). Differentiation of the properties of the branching isozymes from maize (*Zea mays*). *Plant Physiol.* **102**: 1269–1273.
- Hejazi, M., Fettke, J., Haebel, S., Edner, C., Paris, O., Froberg, C., Steup, M., and Ritte, G.** (2008). Glucan, water dikinase phosphorylates crystalline maltodextrins and thereby initiates solubilisation. *Plant J.* **55**: 323–334.
- Hennen-Bierwagen, T.A., Liu, F., Marsh, R.S., Kim, S., Gan, Q., Tetlow, I.J., Emes, M.J., James, M.G., and Myers, A.M.** (2008). Starch biosynthetic enzymes from developing maize endosperm associate in multisubunit complexes. *Plant Physiol.* **146**: 1892–1908.
- Hussain, H., Mant, A., Seale, R., Zeeman, S.C., Hinchliffe, E., Edwards, A., Hylton, C., Bornemann, S., Smith, A.M., Martin, C., and Bustos, R.** (2003). Three isoforms of isoamylase contribute different catalytic properties for the debranching of potato glucans. *Plant Cell* **15**: 133–149.
- Ishizaki, Y., Taniguchi, H., Maruyama, Y., and Nakamura, M.** (1983). Debranching enzymes of potato tubers (*Solanum tuberosum* L.). II. Purification of a pullulanase (R-enzyme) from potato tubers and comparison of its properties with those of the potato amylopectinase. *J. Jpn. Soc. Starch Sci.* **30**: 19–29.
- James, M.G., Robertson, D.S., and Myers, A.M.** (1995). Characterisation of the maize gene *sugary1*, a determinant of starch composition in kernels. *Plant Cell* **7**: 417–429.
- Kaplan, F., and Guy, C.L.** (2005). RNA interference of *Arabidopsis* β -amylase 8 prevents maltose accumulation upon cold shock and increases sensitivity of PSII photochemical efficiency to freezing stress. *Plant J.* **44**: 730–743.
- Kubo, A., Fujita, N., Harada, K., Matsuda, T., Satoh, H., and Nakamura, Y.** (1999). The starch debranching enzymes isoamylase and pullulanase are both involved in amylopectin biosynthesis in rice endosperm. *Plant Physiol.* **121**: 399–409.
- Lu, Y., and Sharkey, T.D.** (2004). The role of amylomaltase in maltose metabolism in the cytosol of photosynthetic cells. *Planta* **218**: 466–473.
- Manners, D.J.** (1991). Recent developments in our understanding of glycogen structure. *Carbohydrate Polymers* **16**: 37–82.
- Matheson, N.K.** (1975). The $\alpha(1-4)(1-6)$ glucans from sweet and normal corns. *Phytochemistry* **14**: 2017–2021.
- Mouille, G., Maddelein, M.-L., Libessart, N., Talaga, P., Decq, A., Delrue, B., and Ball, S.G.** (1996). Preamylopectin processing: A mandatory step for starch biosynthesis in plants. *Plant Cell* **8**: 1353–1366.
- Myers, A.M., Morell, M.K., James, M.G., and Ball, S.G.** (2000). Recent progress toward understanding biosynthesis of the amylopectin crystal. *Plant Physiol.* **122**: 989–997.
- Nakamura, Y., Kubo, A., Shimamune, T., Matsuda, T., Harada, K., and Satoh, H.** (1997). Correlation between activities of starch debranching enzyme and α -polyglucan structure in endosperms of *sugary-1* mutants of rice. *Plant J.* **12**: 143–153.
- Niittylä, T., Messerli, G., Trevisan, M., Chen, J., Smith, A.M., and Zeeman, S.C.** (2004). A previously unknown maltose transporter essential for starch degradation in leaves. *Science* **303**: 87–89.
- Nishi, A., Nakamura, Y., Tanaka, N., and Satoh, H.** (2001). Biochemical and genetic analysis of the effects of amylose-extender mutation in rice endosperm. *Plant Physiol.* **127**: 459–472.
- O’Sullivan, A.C., and Perez, S.** (1999). The relationship between internal chain length of amylopectin and crystallinity in starch. *Biopolymers* **50**: 381–390.
- Posewitz, M.C., Smolinskia, S.L., Kanakagirib, S., Melisb, A., Seiberta, M., and Ghirardia, M.L.** (2004). Hydrogen photoproduction

is attenuated by disruption of an isoamylase gene in *Chlamydomonas reinhardtii*. *Plant Cell* **16**: 2151–2163.

- Rahman, S., Nakamura, Y., Li, Z., Clarke, B., Fujita, N., Mukai, Y., Yamamoto, M., Regina, A., Tan, Z., Kawasaki, S., and Morell, M.** (2003). The sugary-type isoamylase gene from rice and *Aegilops tauschii*: Characterization and comparison with maize and *Arabidopsis*. *Genome* **46**: 496–506.
- Richter, T., Biel, S.S., Sattler, M., Wenck, H., Wittern, K.P., Wiesendanger, R., and Wepf, R.** (2007). Pros and cons: Cryo-electron microscopic evaluation of block faces versus cryo-sections from frozen-hydrated skin specimens prepared by different techniques. *J. Microsc.* **225**: 201–207.
- Roldán, I., Wattebled, F., Lucas, M.M., Delvallé, D., Planchot, V., Jiménez, S., Pérez, R., Ball, S., D'Hulst, C., and Mérida, Á.** (2007). The phenotype of soluble starch synthase IV defective mutants of *Arabidopsis thaliana* suggests a novel function of elongation enzymes in the control of starch granule formation. *Plant J.* **49**: 492–504.
- Scheidig, A., Fröhlich, A., Schulze, S., Lloyd, J.R., and Kossmann, J.** (2002). Down regulation of a chloroplast-targeted β -amylase leads to a starch-excess phenotype in leaves. *Plant J.* **30**: 581–591.
- Smith, A.M., and Zeeman, S.C.** (2006). Quantification of starch in plant tissues. *Nat. Protocols* **1**: 1342–1345.
- Starcher, B.** (2001). A ninhydrin-based assay to quantitate the total protein content of tissue samples. *Anal. Biochem.* **292**: 125–129.
- Takashima, Y., Senoura, T., Yoshizaki, T., Haniada, S., Ito, H., and Matsui, H.** (2007). Differential chain-length specificities of two isoamylase-type starch-debranching enzymes from developing seeds of kidney bean. *Biosci. Biotechnol. Biochem.* **71**: 2308–2312.
- Takeda, Y., Guan, H.P., and Preiss, J.** (1993). Branching of amylose by the branching isoenzymes of maize endosperm. *Carbohydr. Res.* **240**: 253–263.
- Tetlow, I.J., Beisel, K.G., Cameron, S., Makhmoudova, A., Liu, F., Bresolin, N.S., Wait, R., Morell, M.K., and Emes, M.J.** (2008). Analysis of protein complexes in wheat amyloplasts reveals functional interactions among starch biosynthetic enzymes. *Plant Physiol.* **146**: 1878–1891.
- Tetlow, I.J., Wait, R., Lu, Z., Akkasaeng, R., Bowsher, C.G., Eposito, S., Kosar-Hashemi, B., Morell, M.K., and Emes, M.J.** (2004). Protein phosphorylation in amyloplasts regulates starch branching enzyme activity and protein–protein interactions. *Plant Cell* **16**: 694–708.
- Tomlinson, K., and Denyer, K.** (2003). Starch synthesis in cereal grains. *Adv. Bot. Res.* **40**: 1–61.
- Utsumi, Y., and Nakamura, Y.** (2006). Structural and enzymatic characterization of the Isoamylase1 homo-oligomer and the Isoamylase1-Isoamylase2 hetero-oligomer from rice endosperm. *Planta* **225**: 75–87.
- Wattebled, F., Dong, Y., Dumez, S., Delvallé, D., Planchot, R., Berbezy, P., Vyas, D., Colonna, P., Chatterjee, M., Ball, S., and D'Hulst, C.** (2005). Mutants of *Arabidopsis* lacking a chloroplastic isoamylase accumulate phytyglycogen and an abnormal form of amylopectin. *Plant Physiol.* **138**: 184–195.
- Wepf, R., Amrein, M., Bürkli, U., and Gross, H.** (1991). Platinum/iridium/carbon: A high-resolution shadowing material for TEM, STM and SEM of biological macromolecular structures. *J. Microsc.* **163**: 51–64.
- Wong, K.-S., Kubo, A., Jane, J.-L., Harada, K., Satoh, H., and Nakamura, Y.** (2003). Structures and properties of amylopectin and phytyglycogen in the endosperm of *sugary-1* mutants of rice. *J. Cereal Sci.* **37**: 139–149.
- Wu, C.Y., Colleoni, C., Myers, A.M., and James, M.G.** (2002). Enzymatic properties and regulation of ZPU1, the maize pullulanase-type starch debranching enzyme. *Arch. Biochem. Biophys.* **406**: 21–32.
- Yu, T.-S., et al.** (2005). α -Amylase is not required for breakdown of transitory starch in *Arabidopsis* leaves. *J. Biol. Chem.* **280**: 9773–9779.
- Zeeman, S.C., Northrop, F., Smith, A.M., and ap Rees, T.** (1998a). A starch-accumulating mutant of *Arabidopsis thaliana* deficient in a chloroplastic starch-hydrolyzing enzyme. *Plant J.* **15**: 357–365.
- Zeeman, S.C., Smith, S.M., and Smith, A.M.** (2007). The diurnal metabolism of leaf starch. *Biochem. J.* **401**: 13–28.
- Zeeman, S.C., Umemoto, T., Lue, W.-L., Au-Yeung, P., Martin, C., Smith, A.M., and Chen, J.** (1998b). A mutant of *Arabidopsis* lacking a chloroplastic isoamylase accumulates both starch and phytyglycogen. *Plant Cell* **10**: 1699–1711.